

~~Precipitation rather than wind drives the response of East Asian forests to tropical cyclones~~

Tropical cyclones facilitate recovery of forest leaf area from summer droughts in East Asia

Yi-Ying Chen¹ and Sebastiaan Luyssaert²

¹Research Center for Environmental Changes, Academia Sinica, Taipei, 11529, Taiwan

²Faculty of Science, Vrije Universiteit Amsterdam, Amsterdam, 1081, The Netherlands

Correspondence to: Yi-Ying Chen (yiyingchen@gate.sinica.edu.tw)

Abstract. Forests disturbance by tropical cyclones is mostly documented by field studies of exceptionally strong cyclones and satellite-based approaches attributing decreases in leaf area. ~~The biases that come with such approaches~~By starting their analysis from the observed damage, these studies are biased and may, therefore, limit our understanding of the impact of cyclones in general. This study overcomes such biases by ~~starting the analysis from the observed storm tracks rather than the observed damage.~~ Changes in forest leaf area in East Asia were assessed by jointly ~~analyzing~~analysing the cyclone tracks, climate reanalysis, and changes in satellite-based leaf area following the passage of ~~145 ± 42~~140 ± 41 cyclones. Sixty days following their passage, ~~14 ± 6~~18 ± 8 % of the cyclones resulted in a decrease and ~~55 ± 21~~48 ± 18 % showed no change in leaf area compared to nearby forest outside the storm track. For a surprising ~~31 ± 6~~34 ± 7 % of the cyclones, an increase in leaf area was observed. ~~Further analysis revealed that cyclones bringing abundant precipitation to dry forest soils~~Cyclones resulting in summer could relieve water stress within the storm track increasing itshigher leaf area in their affected compared to ~~vegetation outside~~their references area coincided with an atmospheric pressure dipole steering the cyclone towards a region experiencing summer ~~drought caused by the storm track.~~ This observation calls for ~~refining~~same dipole. When the dipole was present ~~day view, the destructive power~~ of cyclones ~~as agents of destruction toward a more nuanced vision that recognizes that cyclones could~~might have ~~minor or even positive effects on leaf area and as such been offset by their abundant precipitation enabling forest canopies in the affected area to recover faster from the drought than canopies in the reference area.~~ This study documents previously undocumented wide-spread antagonist interactions on forest ~~growth.~~leaf area between droughts and tropical cyclones.

Main Text

Each year almost 30 cyclones, about one-third of the world's tropical cyclones, develop over the Pacific Ocean north of the equator (Landsea, 2000) where a subtropical ridge steers them mainly west and northwest towards Eastern Asia, where 90 % make landfall. The majority of the tropical cyclones in the ~~northwestern~~north western Pacific basin develop between June and November (Bushnell et al., 2018) and more than half acquire typhoon strength (WMO, 2017). The four most powerful typhoons in the region since 1999, i.e., Morakot in 2009, Megi in 2010, Haiyan in

33 2013, and another typhoon also named Megi in 2016, claimed over 7,000 lives, left 1,700 missing, and destroyed over
34 10 billion USD worth of infrastructure and crops according to compilations of mostly local news sources (Yang et al.,
35 2014; Bowen, 2016; Lu et al., 2017; OCHA, 2010). Although natural ecosystems, such as forests, have adapted to
36 recurring high wind speeds (Eloy et al., 2017; Louf et al., 2018; Curran et al., 2008), stem breakage is almost
37 unavoidable at wind speeds above 40 m s⁻¹ (Virost et al., 2016) but has been widely reported at wind speeds well below
38 this threshold together with other damage (~~Tang et al., 2003; Chiu et al., 2018; Chang et al., 2020a~~)(Tang et al., 2003;
39 Chiu et al., 2018; Chang et al., 2020). Despite the economic importance of forests in the region (Barbier, 1993; Vickers
40 et al., 2010), an overall assessment of the damage of tropical cyclones on forest resources is still lacking.

41
42 By jointly ~~analyzing~~analysing cyclone tracks (~~JTWC, 2019~~)(Joint Typhoon Warning Center ; JTWC, 2019), climate
43 reanalysis data (~~ECMWF, 2019~~), and(ERA5-Land; ECMWF, 2019), satellite-based proxies of soil dryness (~~Beguiria~~
44 ~~et al., 2014~~)(SPEIbase v2.6; Beguería et al., 2014), land cover (~~ESA, 2017~~)(ESA CCI; ESA, 2017), and leaf area
45 (~~Martins et al., 2020~~)(ESA LAI; Martins et al., 2020), we estimated: (a) the potential forest area damaged by tropical
46 cyclones, (b) the impact of tropical cyclones on leaf area, and (c) the main drivers of this impact. Previous studies
47 attributed decreases in leaf area or related satellite-based indices to different disturbance agents (Ozdogan et al., 2014;
48 Honkavaara et al., 2013; Forzieri et al., 2020), including cyclones (~~Ozdogan et al., 2014; Takao et al., 2014;~~
49 ~~Honkavaara et al., 2013; Forzieri et al., 2020~~)(Takao et al., 2014). A damage-based approach is designed to identify
50 only decreases in leaf area, thus failing to identify events in which tropical cyclones left the leaf area unaltered or even
51 increased it. In contrast, this study starts the analysis from the actual storm tracks which allows for an unbiased
52 assessment of the impact of cyclones on forests (Blanc and Strobl, 2016).

53
54 The land area affected was identified for each of the 580 tropical cyclones that occurred in the study region between
55 1999 and 2018, considering that cyclone-driven damage could only occur within the storm track at locations that
56 experienced high wind speeds ~~and~~or high precipitation. Pixels within the storm track defined as 2, 3 of 4 times the
57 diameter of the cyclone for which ~~the~~threshold values for wind or precipitation were exceeded were classified as
58 affected areas, the remaining pixels in the track served as a cyclone-specific reference area. The uncertainty derived
59 from defining the width of the storm track (Willoughby and Rahn, 2004) and determining which wind speeds and
60 amounts of precipitation could result in damage are accounted for by an ensemble of nine related definitions with
61 different threshold values (**Table A1**). ~~Uncertainties reported in In this study report uncertainties~~ represent the standard
62 deviation across the nine definitions for the affected area and are accounted for in Figs 1, 2, 3, and A2, and Tables A1,
63 A2 and A3.

64
65 Since 1999, ~~224 ± 69 Mha~~2,240,000 ± 690,000 km² of forest in the study region experienced conditions that may have
66 resulted in cyclone-driven damage, at least once every decade (**Fig. 1A1a**). At decadal or longer return intervals, a
67 single cyclone may greatly affect ecosystem functioning, forest structure and species composition of the forest (Xi,
68 2015; Castañeda-Moya et al., 2020). No less than ~~54 ± 26 Mha~~540,000 ± 260,000 km², including 70 % of the tropical

69 forest in the region, experienced potentially damaging conditions at least once per year, and are thus classified as being
70 under chronic wind stress (**Fig. 1A**). ~~Lower estimates~~ **1b**. Estimates from the rain-only definitions closely matched
71 the ~~70 Mha~~ 700,000 km² yr⁻¹ that was reported following a similar approach in which the affected area was defined as
72 a 100 km buffer zone along the storm track (Lin et al., 2020).

73
74 Irrespective of the definition of the affected area, the coefficient of variation of the between-year variation in
75 potentially damaged areas ranged from 15 to 20 % (**Fig. 1B1c**). Excluding the four most powerful typhoons that
76 occurred in the region since 1999 changed the average coefficient of variation from 17 to 16 %. This suggests that the
77 most powerful typhoons make only a small contribution to the total annually potentially affected area in the region. A
78 recent literature review reported, however, that 66 % of the research papers in this area have examined the effects of
79 only about 6 % of the most powerful cyclones (Lin et al., 2020). The relatively small contribution of those events to
80 the potentially damage area suggests that in regions with frequent tropical storms, disturbance ecology would benefit
81 from broadening its scope by examining the effects and recovery of a representative sample of tropical cyclones, rather
82 than focusing on the most devastating events.

83
84 ~~The different definitions of affected area (Table A1) consistently show a high potential for forest damage over island
85 and coastal regions located between 10 and 35 degrees latitude (Fig. 1C). Although damage potential is the outcome
86 of an interplay between cyclone frequency, cyclone intensity and the presence of forests, the high potential in this
87 region is largely driven by the frequency of tropical cyclones (Fig. A1), i.e., two or more cyclones making landfall
88 per year. Depending on how the affected area is defined, there is a second region located between 40 and 50 degrees
89 north with a high potential for storm damage (Fig. 1C). In this region, the potential damage is the outcome of the high
90 forest cover resulting in a strong dependency on the assumed width of the storm track (Fig. A1).~~

91
92 The impact of a tropical cyclone on leaf area was calculated based on the adjusted Hedge's effect size by comparing
93 the change in leaf area before and after the cyclone in the affected area with the change before and after the cyclone
94 in the reference area for each individual cyclone (**Eq. 1**). Using a reference area that is specific to each cyclone means
95 that seasonal dynamics related to leaf phenology and seasonal monsoons ~~can be~~ are accounted for in the effect size,
96 which is a unitless description of the mean change in leaf area normalized by its standard deviation (**Eq. 1**). ~~A~~ Hence,
97 a positive or negative effect size ~~respectively~~ denotes ~~ana~~ a faster increase or a slower decrease in leaf area in the affected
98 area compared to the reference area following the passage of a tropical cyclone.

99
100 A total of 316 ± 22 tropical cyclones or 54 ± 4 % of the storm events under study could not be further analysed (**Table**
101 **A1**) because leaf area index (~~LAI~~) observations were missing from either the affected area, the reference area, or both,
102 thus violating the requirements for calculating the effect size (**Eq. 1**). Of the remaining 264 ± 22 tropical cyclones,
103 only ~~145~~ 42 ~~140~~ ± 41 passed the additional quality ~~checks~~ check necessary to be retained for further analysis in this
104 study: ~~(i) have a less than 0.5 m²·m⁻².e., the~~ difference in the leaf area between the reference and affected area prior

105 to the passage of ~~the~~ storm ~~signifying that should be less than 10 % of the leaf area in the reference area. In other~~
106 ~~words, prior to the storm, the leaf area in the reference area is indeed had to be similar to the leaf area in what will~~
107 ~~become the affected area; and (ii) have an effect size that is larger~~ once the storm passed. Of the 580 cyclones, 31 %
108 ~~was less than the noise of the remotely sensed leaf area-~~class 1, 14 % was classified as class 1, 11 % as class 2, 10 %
109 ~~as class 3, 21 % as class 4, and 13 % as class 5. The distribution of the intensity classes of the sample of 140 ± 41~~
110 ~~cyclones that could be further analysed were similar to the census of the 580 cyclones with 33 % of the retained~~
111 ~~cyclones classified below class 1, 13 % in class 1, 8 % in class 2, 9 % in class 3, 23 % in class 4, and 14 % class 5.~~
112 Despite the loss of around 75 % of the 580 events, the ~~quality control criteria resulted in an sample analysed in this~~
113 ~~study is~~ unbiased ~~sample~~ in terms of ~~wind speed~~ cyclone intensity classes (Fig. A2).

114
115 ~~The effect size of 79 ± 31 events was less than the noise of the remotely sensed change in leaf area suggesting that for~~
116 ~~55 ± 21 % of the cyclones, the change in leaf area 60 days after a cyclone passed was too small to distinguish it from~~
117 ~~the noise of present day remote sensing technology. Nevertheless, ecological theory predicts forest dwarfing in regions~~
118 ~~with high cyclone frequencies~~

119 ~~Tropical cyclones have been widely observed to defoliate and disturb forests because of limb breaking, uprooting,~~
120 ~~stem breakage and landslides following high wind speeds and heavy precipitation (Wang et al., 2013; Uriarte et al.,~~
121 ~~2019; Chambers et al., 2007; Douglas, 1999; Lin et al., 2011).~~ Nevertheless, in this study, only 18 ± 8 % of the
122 ~~observed cyclones resulted in a detectable reduction in leaf area 60 days after their passage as a direct effect of limb~~
123 ~~breakage, uprooting, stem breakage and landslides. For 48 ± 18 % of the cyclones, the change in leaf area 60 days~~
124 ~~after a cyclone passed was so small that it could not be distinguished from the threshold representing no-change.~~
125 ~~Ecological theory predicts forest dwarfing in regions with high cyclone frequencies compared to the longevity of a~~
126 ~~tree,~~ directly through gradual removal of taller trees over many generations (Lin et al., 2020; McDowell et al., 2020)
127 and indirectly through the loss of nutrients (Tang et al., 2003; Lin et al., 2011). Where forest dwarfing has occurred,
128 it might be hard to observe the short-term effects of an individual tropical cyclone on forest structure and function
129 (Mabry et al., 1998). ~~Following the terminology of this study, a neutral effect size over regions with high return~~
130 ~~frequencies would be consistent with structural adaptation to frequent cyclones. Indeed, for regions that experience~~
131 ~~over 4.5 cyclones per year, the mean effect size was almost zero (Fig. A3).~~

132
133 ~~For a surprising 34 ± 7 % of the cyclones an increase or given the way the effect size was calculated, a reduced~~
134 ~~decrease in leaf area was observed, leading to the question which conditions lead to an increase or a reduced decrease~~
135 ~~in leaf area between the affected and reference areas 60 days following the passage of a tropical cyclone? To answer~~
136 ~~this question, two groups of meta-data were compiled for each of the 140 ± 41~~

137 ~~Tropical cyclones have been widely observed to defoliate and disturb forests because of limb breaking, uprooting,~~
138 ~~stem breakage and landslides following high wind speeds and heavy precipitation (Wang et al., 2013; Uriarte et al.,~~
139 ~~2019; Chambers et al., 2007; Douglas, 1999; Lin et al., 2011).~~ Nevertheless, in this study, only 14 ± 6 % of the
140 ~~observed cyclones resulted in a detectable reduction in leaf area as a direct effect of limb breakage, uprooting, stem~~

141 breakage and landslides, 60 days after their passage. On the other hand, for $31 \pm 6\%$ of the cyclones an increase in
142 leaf area was observed, leading to the question: which conditions lead to an increase (or a reduced decrease) in leaf
143 area between the affected and control areas 60 days following the passage of a tropical cyclone?

144
145 To answer this question, two groups of meta-data were compiled for each of the 145 ± 42 tropical cyclones that passed
146 the quality checks, the first group consisting of five characteristics describing the land surface before the passage of a
147 cyclone and the second group containing five characteristics of the cyclone itself (Table A2). Following factorial
148 analysis to identify collinearity between the meta-data in the same group, the explanatory power of the meta-data was
149 quantified as a decrease in the accuracy of a random forest analysis (Fig. 2). The random forest analysis was repeated
150 12 times with different combinations of largely uncorrelated meta-data (Table A3). Each random forest analysis
151 included the effect sizes and meta-data for all nine definitions of affected area to account for this specific source of
152 uncertainty.

153
154 The statistical analysis showed that accumulation of precipitation during the passage of a cyclone over land makes the
155 largest contribution to the accuracy of the random forest analysis. Randomizing this variable decreased the accuracy
156 of the random forest analysis by 209 to 2621 % (Fig. 2). Soil dryness quantified as the standardized precipitation and
157 evapotranspiration The Pacific Japan index (SPEI) for atmospheric pressure at the time of landfall was the second most
158 important variable contributing 21 to 17 % whereas the%. The other meta-data contributed relatively little (-46 to 78
159 %) to the accuracy of the random forest analysis with negative importance indicating that removing the variable from
160 the model improved its performance. Subsequently, the six meta-data with the highest explanatory power were used
161 to build a single regression tree to obtain the environmental drivers and their cut-off values that would best explain
162 the change in leaf area following the passage of a tropical cyclone (Fig. 3). ~~In~~Note that cyclone intensity had a low
163 explanatory power (Fig. 3) which is explained by the observation that positive, neutral and negative effects occurred
164 in all five intensity classes (Fig. A2). The remainder of this report we focus focusses on the unexpected result,
165 i.e., mechanisms underlying the increase or reduced decrease in leaf area following the passage of a tropical cyclone.

166
167 Cyclones bringing abundant precipitation ($\geq 19 (> 32)$ mm) during summer months (i.e., after month 6.5) when the
168 forest soil atmosphere was dry (SPEI \leq under a positive phase of Pacific Japan index (> -0.74028)) resulted dominantly
169 (6056 % to 7069 %) in a leaf area that was $0.5 \text{ m}^2 \text{ m}^{-2}$ higher in the affected compared to the reference area (Fig.
170 3). Given that the passage of the cyclone was often preceded by a summer drought, the observed increase in leaf area
171 along the storm track (Fig. 3) should most likely be interpreted as a faster recovery from the drought in the area
172 affected by the cyclone than in its reference area. The vegetation response was thought to be the outcome of two
173 elements: (a) cyclones making landfall in June, July and August bring 30 to 50 % of the annual precipitation in coastal
174 areas in the study domain (Fig. A4A3) and are thus substantial sources of precipitation. The importance of the
175 precipitation brought by tropical cyclones is confirmed by domain-wide changes in the Standardized Precipitation-
176 Evapotranspiration Index standardized precipitation-evapotranspiration index showing that 10701006 of the 1309

177 ~~(82/1262 (80 %)~~ cyclones increased soil wetness, and (b) given that much of the study domain has a monsoon climate
178 with relatively little rain in the fall and winter months; ~~(Chou et al., 2009)~~, the implication is that summer droughts
179 might, for evergreen vegetation, have lasting effects until the next growing season ~~(Chou et al., 2009)~~ unless the
180 drought was ended before the dry season begins. Cyclones, especially those later in summer could bring the
181 precipitation to end summer droughts. For unless the drought is ended before the dry season begins.

182
183 An increase in leaf area or a reduced decrease, following the passage of a tropical cyclone, thus requires three
184 conditions to co-occur: (a) a dry spell, (b) a cyclone making landfall in the region experiencing the dry spell, and (c)
185 the cyclone bringing abundant precipitation to mitigate the soil dryness. At first sight, meeting all three conditions at
186 the same time seems unlikely, however, for the mid-latitudes, including Korea, China, Taiwan, and Japan, dry
187 summers see an increase in the number of tropical cyclones making landfall which often end the summer drought
188 (Yoo et al., 2015). In South Korea, for example, at least 43 % but possibly as much as 90 % of the summer droughts
189 in coastal regions were abruptly ended by a tropical cyclone (Yoo et al., 2015). Based on our analysis of the
190 Standardized Precipitation Evapotranspiration Index, 214standardized precipitation-evapotranspiration index, at least
191 210 of the ~~1309 (16/1262 (17 %)~~ tropical cyclones in East Asia ended a drought.

192
193 ~~An increase in leaf area, following the passage of a tropical cyclone, thus requires three conditions to co-occur: (a) a~~
194 ~~dry spell, (b) a cyclone making landfall in the region experiencing the dry spell, and (c) the cyclone bringing abundant~~
195 ~~precipitation to mitigate the soil dryness. Meeting all three conditions at the same time seems unlikely unless there is~~
196 ~~a physical relationship between summer droughts (a) and tropical cyclones (b). During dry years, a meridional dipole~~
197 ~~system has been observed~~The co-occurrence of dry spells and tropical cyclones has been linked to a meridional dipole
198 system in the mid-latitude regions of East Asia with a high pressure system in the region of 40-50 N and 150-~~160E~~160
199 E where it is causing the dry spell, and the low pressure system in the region of 20-~~30N~~30 N and 120-~~150N~~150 E.
200 When such a dipole exists, tropical cyclones generated from the monsoon trough over the West Pacific Ocean are
201 steered through the trough in between the high- and low-pressure systems towards and then along the coast of East
202 Asia ~~(Choi et al., 2010)~~(Choi et al., 2010). While travelling along the edges of the high pressure system, the tropical
203 cyclone may disturb the circulation, resulting in an unfavourable environment to sustain the dipole (Choi et al., 2011;
204 Kubota et al., 2016) and bringing precipitation to the dry region that was under the high pressure system.

205
206 ~~By studying a representative sample of tropical cyclones (in terms of storm intensity) (Fig. A2), we have shown that~~
207 ~~over half of the tropical cyclones, i.e., 55 ± 21 %, caused little to no damage to forest leaf area, suggesting that forest~~
208 ~~dwarfing is a general structural adaption in the study region. Moreover, a third, i.e., 31 ± 6 % of the cyclones in East~~
209 ~~Asia resulted in an increase in forest growth, because these storms relieved water stress within their track or even~~
210 ~~ended summer droughts. The observed frequency of positive vegetation responses to cyclones suggests that the present~~
211 ~~day vision of cyclones as agents of destruction (Altman et al., 2018; Negrón-Juárez et al., 2010; Nelson et al., 1994)~~
212 ~~should be refined toward a recognition that, depending on the environmental conditions prior to the storm and the~~

213 characteristics of the storm itself, cyclones could also have limited destructive effects (Lin et al., 2020) or even positive
214 effects on forest growth (Castañeda Moya et al., 2020; Chang et al., 2020b). As both cyclones (Mei and Xie, 2016)
215 and droughts (Zhao and Dai, 2017) are expected to continue to intensify with global warming, the net direct effect
216 through relieved water stress and indirect effect through possible connections with fire activities (Stuivenolt Allen et
217 al., 2021) remains highly uncertain.

218 As suggested by the random forest analysis (Fig. 2), analysing the atmospheric pressure separately for cyclones that
219 resulted in no change, an increase or a decrease in leaf area (Fig. 4) showed that tropical cyclones that were followed
220 by an increase or reduced decrease in leaf area coincided with a meridional dipole (Fig. 4b). Moreover, the genesis of
221 tropical cyclones that were followed by a decrease in leaf area, occurred under very different atmospheric conditions
222 compared to cyclones followed by an increasing leaf area. A relationship between the atmospheric system causing
223 summer droughts, tropical cyclones and their subsequent impact on leaf areas, suggest that whether more drought
224 damage is to be expected in the future will not only depend on an increase in drought frequency and intensity but will
225 in part be determined by the exact weather system that is causing the drought. Although the co-occurrence of droughts
226 and cyclones has previously been demonstrated (Choi et al., 2011; Kubota et al., 2016), we believe to be the first to
227 document its large-scale antagonist effect on forest leaf area.

229 By studying a representative sample of tropical cyclones in terms of storm intensity (Fig. A2), we have shown that
230 almost half of the tropical cyclones, i.e., 48 ± 18 %, caused little to no damage to forest leaf area, suggesting that forest
231 dwarfing is a general structural adaption in the study region. Moreover, a third, i.e., 34 ± 7 % of the cyclones in East
232 Asia resulted in an increase or reduced decrease in forest growth, because these storms relieved water stress within
233 their track or even ended summer droughts. The observed frequency of positive vegetation responses to cyclones
234 suggests that the present day vision of cyclones as agents of destruction (Altman et al., 2018; Negrón-Juárez et al.,
235 2010, 2014) should be refined toward a recognition that, depending on the environmental conditions prior to the storm
236 and the atmospheric conditions leading to the genesis of the tropical cyclone, cyclones frequently facilitate the
237 recovery of forest leaf area and as such dampen the effects of summer droughts.

239 **Materials and Methods**

240 **Cyclone track and track diameter**

241 Since 1945, tropical cyclones in the Western North Pacific Ocean have been tracked and their intensity recorded by
242 the Joint Typhoon Warning Center (JTWC). The track data shared by the [JTWC Joint Typhoon Warning Center](#) consist
243 of quality-controlled six-hourly geolocation observations of the ~~center~~[center](#) of the storm with the diameter of the
244 storm being a proxy for its intensity (~~JTWC, 2019~~)([JTWC, 2019](#)). For the period under consideration, from 1999 to
245 2018, the geolocations and diameters are the output of the Dvorak model (Dvorak, 1984; Dvorak et al., 1990) derived
246 from visible and infrared satellite imagery. Storm diameters are available starting from January 2003. Prior to this date

247 a generic diameter of 100 km (Lin et al., 2020) is used in this study. Linear interpolation of the six-hourly track data
248 resulted in hourly track data to fill in any gaps in the mapping of the cyclone track.

249
250 In this study, we focus on East Asia which, given the absence of natural boundaries, is defined as the land contained
251 within the ~~northwestern~~north western Pacific basin that, according to the JTWC Joint Typhoon Warning Center
252 stretches from 100 to 150 degrees east and 0 to 60 degrees north. The JTWC Joint Typhoon Warning Center compiled
253 track and intensity data for 580 tropical cyclones between 1999 and 2018 in the ~~northwestern~~north western Pacific
254 basin. A shorter time series (1999 to 2018) than the entire length of time available (1945 to 2018) was
255 ~~analyzed~~analysed due to the more limited availability of the leaf area index (~~LAI~~) data which had to be jointly
256 ~~analyzed~~analysed with the track and intensity data to quantify the impact of cyclones on natural ecosystems.

257 258 **Area affected by individual cyclones**

259 The land area thought to be affected by a specific cyclone as well as the reference area for each of the 580 cyclones
260 that occurred in the study area between 1999 and 2018 were identified based on nine different but related definitions
261 (**Table A1**). Each definition comprises a combination of at least two out of three criteria, e.g., the diameter of the
262 cyclone, the maximum wind speed at each location during the passage of the cyclone and accumulated precipitation
263 at each location during the passage of the cyclone. Each forested pixel within each individual storm track was classified
264 as either affected area or reference area based on these nine definitions. Differences in the results coming from
265 differences in the definitions were used throughout the analysis to estimate semantic uncertainties. Uncertainties
266 related to the estimated diameter of the cyclone, wind speed and precipitation data were not accounted for in the
267 calculation of the affected and reference areas because they were thought to be smaller than the uncertainty coming
268 from differences in the definitions themselves.

269
270 The underlying assumption behind the definitions is that forests can only be affected by a specific cyclone if they are
271 located along its storm track. The minimum width of each storm track is the diameter of the cyclone as reported by
272 the ~~JTWC~~Joint Typhoon Warning Center. Following the observation that over the ocean, the actual wind speed
273 exceeds the critical wind speed for stem breakage or uprooting (i.e., 17 m s⁻¹ ref. Chen et al., 2018) over a distance of
274 at least three times the diameter of the cyclone (Willoughby and Rahn, 2004), the minimum width of a storm track in
275 which cyclone-related forest damage could occur is defined as three times the diameter recorded by the JTWC Joint
276 Typhoon Warning Center although wind speeds drop dramatically when cyclones make land fall (Kaplan and Demaria,
277 2001). The minimum width of a storm track over land should, therefore, be reduced compared to the observations
278 over the ocean. This study used three different widths to define a storm track, i.e., two, three or four times the recorded
279 diameter (**Table A1**).

280
281 Being located within the track of a specific cyclone is essential but not sufficient for damage to occur. Within a storm
282 track, only forested pixels that experienced high wind speeds or high precipitation were counted as in the potentially

283 affected area. Forest pixels that were located within the storm track but did not experience high wind speeds or high
284 precipitation were counted as in the reference area. Note that to better account for the uncertainties arising from this
285 approach, the threshold values for wind speed and precipitation were ~~also~~ increased as the track diameter increased
286 (Table A1). For a narrow storm track it is reasonable to assume that there would be damage shown in all pixels except
287 those where wind speed or precipitation did not exceed a relatively low threshold value. For wide storm tracks the
288 opposite applies; it is reasonable to assume that few of the pixels would show damage except where wind speed or
289 precipitation exceeded relatively high threshold values.

290
291 ~~Data sources for the geolocation and diameter of an individual cyclone are described in detail in ‘Cyclone track and~~
292 ~~diameter’.~~ Wind speed and precipitation data were extracted from the ERA5-Land reanalysis data for land (ECMWF,
293 2019). The ERA5-Land reanalysis dataset has a spatial resolution of 9 km x 9 km and a time step of 1 hour. It is the
294 product of a data assimilation study conducted with the H-TESEL scheme by ERA5 IFS Cy45r1 and nudged by
295 climatological observations (ECMWF, 2018). The Cy45r1 reanalysis dataset shows statistically neutral results for the
296 position error of individual cyclones (ECMWF Confluence Wiki: Implementation of IFS cycle 45r1). The spatial
297 representation of the reanalysis data is reported to compare ~~favorably~~favourably with observational data (Chen et al.,
298 2021) outside the domain of this study. No reports on similar tests for the current study domain, i.e., East Asia, were
299 found. Furthermore, land cover maps released through the European Space Agency’s ~~(ESA’s)~~ Climate Change
300 Initiative (ESA, 2017) were used to restrict the analysis to forests. The ~~CCI~~Climate Change Initiative maps integrate
301 observations from several space-borne sensors, including MERIS, SPOT-VGT, AVHRR, and PROBA-V, into a
302 continuous map with a 300 m resolution from 1994 onwards.

303
304 Wind speed and precipitation data were spatially disaggregated and temporally aggregated to match the spatial and
305 temporal resolution of the ~~ESA~~-leaf area index (~~LAI~~) product (see below). Maximum wind speed and accumulative
306 precipitation were aggregated over time steps to match the 10-day resolution of the ~~ESA-LAI~~leaf area index product.
307 We preserved the temporal resolution of the land cover map but aggregated ~~the~~its spatial resolution from 300 m to 1
308 km to match the resolution of the ~~ESA-LAI~~leaf area index product. During aggregation, the majority of land cover at
309 the 300 m resolution was assigned to the 1 km pixel resolution.

310
311 ~~The oceanic Nino index (ONI) was retrieved from NOAA (NINO SST INDICES (NINO 1+2, 3, 3.4, 4; ONI AND~~
312 ~~TNI), 2019). The oceanic Nino index was calculated and defined by comparing the 3-month running mean sea surface~~
313 ~~temperature over the region from 5 degrees north to 5 degrees south and from 170 degrees west to 120 degrees west~~
314 ~~with the 30-year climatology of sea surface temperature over the same region (Trenberth and Stepaniak, 2001; The~~
315 ~~climate data guide: Nino SST indices (Nino 1+2, 3, 3.4, 4; ONI and TNI)). A monthly seasonal oceanic Nino index~~
316 ~~was used in this study. According to this method, El Nino events are characterized by an oceanic Nino index exceeding~~
317 ~~0.5 K and La Nina events by an oceanic Nino index below 0.5 K. These thresholds relate to a warmer or a cooler~~
318 ~~ocean state in the central tropical Pacific.~~

319
320
321
322
323
324
325
326
327
328
329
330
331
332
333
334
335
336
337
338
339
340
341
342
343
344
345
346
347
348
349
350
351
352

Impact on leaf area of an individual cyclone

Version 2 of [ESA's European Space Agency's](#) Climate Change Initiative product was used to calculate leaf area (LAI) in this study. The product has a 1 km spatial resolution, a 10-day temporal resolution, and is available from 1999 onwards. The default [LAIleaf area index](#) product is distributed as a composite image using at least six valid observations on a pixel within a 30-day moving window (Verger et al., 2014). The composite image is drawn from satellite-based observations of the surface reflectance in the red, near-infrared, and shortwave infrared from SPOT-VGT (from 1999 to May 2014) and PROBA-V (from June 2014 to present). Gaps in missing observations are filled by the application of a relationship between local weather and [LAI dynamics](#). ~~Gap filling resulted in errors on the LAI estimates of less than 0.18 (ref. (Martins et al., 2020)). The spatiotemporal resolution of the LAIleaf area index dynamics. Gap filling resulted in errors on the leaf area index estimates of less than 0.18 (Martins et al., 2017). The spatiotemporal resolution of the leaf area index~~ products was the coarsest of all data products used and therefore determined the spatiotemporal resolution of the analysis as a whole. Moreover, the availability of the [LAIleaf area index](#) product determined the starting date for the study.

The impact of cyclones on leaf area was calculated by comparing the change in leaf area before and after the cyclone in the affected area with changes before and after the cyclone in the reference area for each individual cyclone. In this approach, the reference area serves as the control for the affected area, given that reference area and the affected area may have a different size, the adjusted Hedge's effect size (Rustad et al., 2001) can be used to calculate the effect size of an individual cyclone on leaf area (Eq. 1). Using a reference area that is specific to each cyclone's seasonal dynamics, such as leaf phenology, is accounted for in the effect size. Effect size is thus a unitless quantifier which describes the mean change in state, obtained by normalizing the mean difference in leaf area with the standard deviation (Eq. 1). A positive or negative [Effect size](#) value indicates, respectively, an increase or decrease in leaf area following the passage of a cyclone:

$$ES = \frac{(\overline{LAI}_{bef} - \overline{LAI}_{aft})_{aff} - (\overline{LAI}_{bef} - \overline{LAI}_{aft})_{ref}}{\sigma} \quad [1]$$
$$ES = \frac{(\overline{LAI}_{bef} - \overline{LAI}_{aft})_{aff} - (\overline{LAI}_{bef} - \overline{LAI}_{aft})_{ref}}{\sigma} \quad [1]$$

where ES is the event-based effect size for leaf area. The upper bar represents the mean of [LAIleaf area index](#) in either the reference (ref) or the affected (aff) area. The subscripts ref and aff denote the observation dates before and after the cyclone; σ denotes the standard deviation of all observations within the storm track. Given the 10-day frequency of the ESA [LAIleaf area index](#) product, two [LAIleaf area index](#) maps are used for the calculation of the [Effect size](#), one to characterize the [LAIleaf area index](#) 1 to 10 days before the cyclone and the other to characterize the [LAIleaf area index](#) 60 to 70 days after the cyclone. To distinguish between the affected and reference areas the effect sizes

353 were calculated for each event using the nine definitions. After applying the quality control criteria (see below) a
354 different number of events was available for each definition (**Table A1**).

355
356 ~~The 60-day time frame was a compromise to avoid excessive data gaps in the LAI product when using a composite
357 LAI product. Because the LAI product reports LAI values within a 60-day window, the analysis had to be refined so
358 that this 60-day window never included the cyclone. The offset between the cyclone and a LAI observation from the
359 composite ESA LAI product was calculated by subtracting the date of the cyclone from the last observation date of
360 the LAI composite data before the cyclone or first observation date of the LAI composite data after the cyclone. Pixels
361 with a negative offset indicated that the composite data were likely to include observations from both before and after
362 the cyclone and were therefore discarded in the calculations of the effect size.~~

363
364 Starting the analysis from the actual storm tracks, as was the case in this study, allows for an unbiased assessment of
365 the impact of cyclones on forests (Blanc and Strobl, 2016), ~~in contrast to studies that attribute decreases in leaf area
366 or related satellite-based indices to different disturbance agents including cyclones (Ozdogan et al., 2014; Takao et al.,
367 2014; Honkavaara et al., 2013; Forzieri et al., 2020). By design, the latter approach is not capable of identifying neutral
368 or positive impacts of cyclones on leaf area.~~

369
370 **Quality control**
371 ~~The, in contrast to studies that attribute decreases in leaf area or related satellite-based indices to different disturbance
372 agents (Ozdogan et al., 2014; Honkavaara et al., 2013; Forzieri et al., 2020) including cyclones (Takao et al., 2014).
373 By design, the latter approach is not capable of identifying neutral or positive impacts of cyclones on leaf area. As
374 positive effects were not limited to the cyclones from a low intensity class (**Fig. A2**), the intensity class had little
375 explanatory power (**Fig. 2**) making a systematic bias towards positive effect sizes caused by low intensity cyclones
376 unlikely. Given the 60-day time window, our method is more likely to be biased towards detecting no changes in leaf
377 area than detecting positive or negative changes in leaf area.~~

378
379 ~~A meaningful effect size relies on the change in the reference area to evaluate whether the change in leaf area in the
380 affected area is faster, similar or slower. The way the effect size is calculated thus accounts for phenological changes
381 in leaf area. If the reference area would not be used in the calculation of the effect size, the change in leaf area over
382 the affected area would mostly represent leaf phenology especially if the 60-day window includes the start or the end
383 of the growing season, and would thus be unsuitable to address the question at hand.~~

384
385 ~~As this study aims to quantify changes in leaf area index, it could not make use of gap filled leaf area index values
386 which would level off such changes. Furthermore, calculating the effect size required leaf area index estimates before
387 the passage of the cyclone in the reference and soon-to-be affected area and leaf area index estimates after the passage
388 of the cyclone in the reference and affected area. The 60-day time frame was a compromise to avoid excessive data~~

gaps in the leaf area index product when using the composite leaf area index product. Because the leaf area index product reports leaf area index values within a 60-day window, the analysis had to be refined so that this 60-day window never included the cyclone. The offset between the cyclone and a leaf area index observation from the composite leaf area index product was calculated by subtracting the date of the cyclone from the last observation date of the leaf area index composite data before the cyclone or first observation date of the leaf area index composite data after the cyclone. Pixels with a negative offset indicated that the composite data were likely to include observations from both before and after the cyclone and were therefore discarded in the calculations of the effect size.

The calculation of the effect size assumes having a similar LAI/leaf area index between the area that will become the affected area and the area that will become the reference area after the passage of a cyclone. If the absolute difference in LAI/leaf area index between the reference and the affected area was over 0.25 but less than 0.25, 10 %, the effect size calculated for this event was included in subsequent analyses. This can be formalized as:

$$\left| \frac{\overline{LAI}_{\text{beff}}}{\overline{LAI}_{\text{beref}}} - 1 \right| < 0.1 \quad [2]$$

Where the 0.25 represents the 10 % threshold was derived through error propagation by considering that “similar LAI” implies that the difference in LAI that was guided by the observed relationship between the reference and affected area should be zero before the event. The uncertainty from gap filling satellite based LAI products, i.e., 0.18 (ref. (Martins et al., 2020)) was used to derive a reasonable threshold. Given that each LAI measurement may come remotely-sensed leaf area and its deviation to ground truth data for leaf areas of 5 m² m⁻² or below (Fig. 26 in Jorge, 2020). This quality control criterion reflects the idea that prior to the passage of a tropical cyclone, the LAI needs to be similar in what will become the reference and affected area. If not, changes in leaf area following the passage of the cyclone cannot be assigned to its passage.

Following the passage of a tropical cyclone, a change in LAI of less than 10% before and after the passage of the cyclone was, in line with an uncertainty of 0.18 the difference between two such measurements comes the quality control criterion, considered to be too small to be considered substantial. Such events were classified as cyclones with an uncertainty of 0.25 ($\sqrt{0.18^2 + 0.18^2}$), a neutral effect size. This classification was formalized as:

The uncertainty of ES calculation through error propagation in equation (Eq. 1) is:

$$\delta ES = |ES| * \sqrt{\left(\frac{\delta X}{X}\right)^2 + \left(\frac{\delta Y}{Y}\right)^2}, \quad [2]$$

where X is the nominator and Y is the denominator of Eq. 1. Given that each LAI observation is assumed to have an uncertainty of 0.18, δX is constant at 0.36. The δY can be calculated by $\sqrt{n * (0.18)^2/n}$, where n is the number of

available observations. For each event, the quality of the ES calculation was examined by comparing the actual ES to its uncertainty δES . Events for which $ES < \delta ES$ were not further analyzed. Events with an effect sizes between 0.18 and 0.18 were classified as neutral.

$$|(\overline{LAI}_{bef} - \overline{LAI}_{aft})_{aff} - (\overline{LAI}_{bef} - \overline{LAI}_{aft})_{ref}| < 0.1 * (\overline{LAI}_{bef})_{ref} \quad [3]$$

Multivariate analysis

Each tropical cyclone was characterized by its: (1) latitude of landfall (degrees); (2) intensity of the tropical cyclone ($m s^{-1}$); (3) month of landfall; (4) maximum wind speed during passage over land ($m s^{-1}$); (5) accumulated rainfall during passage over land (mm); (6) accumulated rainfall on land 30 days prior to landfall of the cyclone (mm); (7) affected area during passage over land ($Mha km^2$); (8) leaf area 30 days prior to landfall ($m^2 m^{-2}$); (9) Standardized Precipitation Evapotranspiration Index (SPEI) ($mm mm^{-1}$) as a drought proxy; and (10) oceanic Nino Pacific Japan index the month of landfall ($K-Pa Pa^{-1}$). These characteristics were calculated as the average along the trajectory of the cyclone.

Characteristics 1 to 4 were retrieved from the JFWC Joint Typhoon Warning Center database as detailed in ‘Cyclone track and track diameter’. Characteristics 5 to 6 were retrieved from the ERA5-Land reanalysis data for land (ECMWF, 2019) and characteristic 7 from the analysis combining cyclone track, cyclone diameter and ERA5-Land reanalysis, as explained in ‘Area affected by individual cyclones’. Characteristic 8 was taken from the LAI leaf area index analysis as explained in ‘Impact on leaf area of an individual cyclone’. For characteristic 9, the Standardized Precipitation Evapotranspiration Index with a half degree by half degree spatial resolution and a 10 day temporal resolution was used and combined with the cyclone masks created in ‘Area affected by the individual cyclone’. Characteristic 10, the oceanic Nino index, was retrieved from NOAA (NINO SST INDICES (NINO 1+2, 3, 3.4, 4; ONI AND TNI), 2019). Pacific Japan index, was calculated from ERA5 hourly reanalysis (Hersbach et al., 2018). Details on the calculation of characteristics 9 and 10 are provided in subsequent sections.

The

These ten characteristics were separated into two groups describing the condition of the land and ocean prior to the event (“prior conditions” or PC group) and the characteristics of the tropical cyclone itself (“tropical cyclone characteristic” or TCC group). The prior conditions group contained: pre-event LAI leaf area index, pre-event drought state, pre-event accumulative rainfall, oceanic Nino index, and month. Characteristics such as maximum wind speed, accumulative rainfall, cyclone intensity, affected area, and latitude were used to describe the cyclone itself. (Table A2).

Factor analysis (Revelle, 2017) was used to reveal the collinearity among the selected variables in the “prior conditions” and “tropical cyclone characteristic” group (Table A2). Collinearity was used to create 12 sets Factor analysis (Grice, 2001) was used to reveal the collinearity among the selected variables in the prior conditions and tropical cyclone

characteristic group (Table A2). Collinearity was used to create 12 sets (4 x 3) of mostly independent characteristics (Table A3) which were used as the input for a random forest tree to identify the characteristics that best explained the effect size for LAI leaf area index. The random forest analysis was repeated for each of the 12 sets, but limited to four-layer random forest trees, to identify the importance of the environmental variables on the tropical cyclone effect size (not shown). Finally, to reduce the collinearity of the input variables, only the six variables with the highest explanatory power accuracy in the random forest were used to create a single decision tree which is shown in Fig. 3. For this, the recursive partitioning approach was used with a maximum of fivefour levels and a minimum of 20 samples in each node provided by the R-rpart package (Therneau et al., 2019).

Drought analysis

~~The Standardized Precipitation Evapotranspiration Index (SPEI)~~The standardized precipitation evapotranspiration index, is a proxy index for drought that represents the climatic water balance and was used to assess the drought of a forest soil before and after the passage of an individual tropical cyclone. The standardized precipitation evapotranspiration index data between 1999 and 2018 were retrieved from the Global Standardized Precipitation and Evapotranspiration Index ~~data used in this study were retrieved from the Global SPEI database~~Database (SPEIbase v2.6 (Beguería et al., 2014)), which is based on the CRU TS v.4.03 dataset (Harris et al., 2020). In this study, the temporal resolution of the data was preserved but the spatial resolution was regridded from the original half-degree to 1 km to match the resolution of the ESA LAI leaf area index product. The contribution of an individual tropical cyclone to ending a drought was evaluated by comparing the SPEI standardized precipitation and evapotranspiration index from affected and reference areas through the following equation:

$$\delta SPEI = (SPEI_{imon})_{aff} - (SPEI_{imon})_{ref}, \quad [3]$$

$$\delta SPEI = (SPEI_{imon})_{aff} - (SPEI_{imon})_{ref}, \quad [3]$$

where $\delta SPEI$ is the event-based change in ~~drought~~standardized precipitation and evapotranspiration index. A positive or negative $\delta SPEI$ respectively denotes an increase or decrease in available water resources following the passage of a tropical cyclone. The subscription *imon* represents the integration time of available water resources in the calculation of the SPEI standardized precipitation and evapotranspiration index either in the reference (*ref*) or the affected (*aff*) area which are defined in previous section. The same time window, i.e., 60-days, was applied for the calculation of $\delta SPEI$ and event-based effect size for LAI leaf area index.

Atmospheric analysis

The Pacific Japan index was calculated by comparing the difference of the 3-month running mean atmospheric pressure anomaly from Yokohama in Japan (35 N, 155 E) with Hengchun in Taiwan (22.5 N, 125 E) (Kubota et al.,

495 2016) with the 20 year climatology from 1999 to 2019. A monthly Pacific Japan index was used in this study and the
496 pressure data were retrieved from ERA5 (Hersbach et al., 2018).

497
498 The Pacific Japan index for the month of the passage of each tropical cyclone were stratified according to the impact
499 (given by the effect size) of the cyclone on forest leaf area. Mean absolute atmospheric pressure field and leaf area
500 were calculated for those cyclones with a neutral effect size on leaf area (Fig. 4a). Changes in pressure field and leaf
501 area were calculated for both cyclones with a positive and negative impact on leaf area (Fig. 4b & c).

504 **Acknowledgments**

505 Y.Y.C. would like to thank the National Center for High-performance Computing (NCHC) for sharing its
506 computational resources and data storage facilities. Y.Y.C. was funded through the Ministry of Science and
507 Technology (grant MOST 109-2111-M-001-011 and grant MOST 110-2111-M-001 -011).

509 **Data availability**

511 R-Scripts and ~~all input data~~ ~~to~~for performing the analysis and creating the plots can be found ~~in the following web-~~
512 ~~based~~ ~~repository~~at https://github.com/ychenatsinca/LAI_STUDY_EA_V1/releases/tag/v1 and
513 <https://doi.org/10.5281/zenodo.6459795>. The database of event-based effect sizes, surface properties and cyclone
514 properties for each of the ~~13091262~~ events (i.e., ~~145 ± 42140 ± 41~~ unique tropical cyclones ~~analyzed~~~~analysed~~ for nine
515 related definitions) can be accessed at: <http://YYCdb.synology.me:5833/sharing/MqA4YFBHk>
516 [https://myspace.sinica.edu.tw/public.php?service=files&t=e2vJFnIASIdGgtvnfcqcXAa51-](https://myspace.sinica.edu.tw/public.php?service=files&t=e2vJFnIASIdGgtvnfcqcXAa51-aTCheljUgAJXk2mHjoZ1thVek&W9yeJx13GeHb)
517 [aTCheljUgAJXk2mHjoZ1thVek&W9yeJx13GeHb](https://myspace.sinica.edu.tw/public.php?service=files&t=e2vJFnIASIdGgtvnfcqcXAa51-aTCheljUgAJXk2mHjoZ1thVek&W9yeJx13GeHb)

518 **Author Contributions**

520 ~~Y.Y.C. and S.L. designed the study. Y.Y.C. investigated and visualized the results. Y.Y.C. and S.L. contributed to the~~
521 ~~interpretation of the results. S.L. wrote the original draft. S.L. and Y.Y.C. reviewed and edited the manuscript.~~

522
523 ~~**Competing Interest Statement:** The authors declare no competing interests.~~

524 **References**

526 Altman, J., Ukhvatkina, O. N., Omelko, A. M., Macek, M., Plener, T., Pejcha, V., Cerny, T., Petrik, P., Srutek, M.,
527 Song, J.-S., Zhmerenetsky, A. A., Vozmishcheva, A. S., Krestov, P.V., Petrenko, T. Y., Treydte, K., and Dolezal, J.:
528 Poleward migration of the destructive effects of tropical cyclones during the 20th century, Proc. Natl. Acad. Sci., 115,
529 11543–11548, <https://doi.org/10.1073/pnas.1808979115>, 2018.

530 Barbier, E. B.: Economic aspects of tropical deforestation in Southeast Asia, *Glob. Ecol. Biogeogr. Lett.*, 3, 215,
531 <https://doi.org/10.2307/2997771>, 1993.

532 Beguería, S., Vicente-Serrano, S. M., Reig, F., and Latorre, B.: Standardized precipitation evapotranspiration index
533 (SPEI) revisited: Parameter fitting, evapotranspiration models, tools, datasets and drought monitoring, *Int. J. Climatol.*,
534 34, 3001–3023, <https://doi.org/10.1002/joc.3887>, 2014.

535 Blanc, E. and Strobl, E.: Assessing the impact of typhoons on rice production in the Philippines, *J. Appl. Meteorol.*
536 *Climatol.*, 55, 993–1007, <https://doi.org/10.1175/jamc-d-15-0214.1>, 2016.

537 Bowen, T.: Social Protection in the Philippines “Emergency cash transfer” program in the Philippines, 1–16, 2016.

538 Bushnell, J. M., Cherrett, R. C., and Falvey, R. J.: Annual Tropical Cyclone Report 2018, 147pp., 2018.

539 Castañeda-Moya, E., Rivera-Monroy, V. H., Chambers, R. M., Zhao, X., Lamb-Wotton, L., Gorsky, A., Gaiser, E. E.,
540 Troxler, T. G., Kominoski, J. S., and Hiatt, M.: Hurricanes fertilize mangrove forests in the Gulf of Mexico (Florida
541 Everglades, USA), *Proc. Natl. Acad. Sci. U. S. A.*, 117, 4831–4841, <https://doi.org/10.1073/pnas.1908597117>, 2020.

542 Chambers, J. Q., Fisher, J. I., Zeng, H., Chapman, E. L., Baker, D. B., ~~and Hurtt and Hurtt~~, G. C.: Hurricane Katrina’s
543 carbon footprint on U.S. Gulf coast forests, *Science*, 318, 1107–1107, <https://doi.org/10.1126/science.1148913>, 2007.

544 Chang, C.-T., Lee Shaner, P.-J., Wang, H.-H., and Lin, T.-C.: Resilience of a subtropical rainforest to annual typhoon
545 disturbance: Lessons from 25-year data of leaf area index, *For. Ecol. Manage.*, 470–471, 118210,
546 <https://doi.org/10.1016/j.foreco.2020.118210>, ~~2020a~~2020.

547 ~~Chang, C. T., Shih, Y. T., Lee, L. C., Lee, J. Y., Lee, T. Y., Lin, T. C., and Huang, J. C.: Effects of land cover and
548 atmospheric input on nutrient budget in subtropical mountainous rivers, northeastern taiwan, 12,
549 <https://doi.org/10.3390/w12102800>, 2020b.~~

550 Chen, Y.-Y., Gardiner, B., Pasztor, F., Blennow, K., Ryder, J., Valade, A., Naudts, K., Otto, J., McGrath, M. J.,
551 Planque, C., and Luyssaert, S.: Simulating damage for wind storms in the land surface model ORCHIDEE-CAN
552 (revision 4262), *Geosci. Model Dev.*, 11, 771–791, <https://doi.org/10.5194/gmd-11-771-2018>, 2018.

553 Chen, Y., Sharma, S., Zhou, X., Yang, K., Li, X., Niu, X., Hu, X., and Khadka, N.: Spatial performance of multiple
554 reanalysis precipitation datasets on the southern slope of central Himalaya, *Atmos. Res.*, 250, 105365,
555 <https://doi.org/10.1016/j.atmosres.2020.105365>, 2021.

556 Chiu, C.-M., Chien, C.-T., Nigh, G., and Chung, C.-H.: Influence of climate on tree mortality in Taiwan (Taiwania
557 *cryptomerioides*) stands in Taiwan, *New Zeal. J. For. Sci.*, 48, <https://doi.org/10.1186/A40490s40490-018-0111-0>,
558 2018.

559 Choi, K.-S., Wu, C.-C., and Cha, E.-J.: Change of tropical cyclone activity by Pacific-Japan teleconnection pattern in
560 the western North Pacific, *J. Geophys. Res. Atmos.*, 115, 1–13, <https://doi.org/10.1029/2010JD013866>, 2010.

561 Choi, K.-S., Kim, D.-W., and Byun, H.-R.: Relationship between summer drought of mid-latitudes in East Asia and
562 tropical cyclone genesis frequency in the Western North Pacific, in: *Advances in Geosciences (A 6-Volume Set)*,
563 edited by: Satake, K. and Wu, C.-C., World Scientific Publishing Co. Pte. Ltd., 1–13,
564 https://doi.org/10.1142/9789814355315_0001, 2011.

565 Chou, C., Huang, L.-F., Tseng, L., Tu, J.-Y., and Tan, P.-H.: Annual cycle of rainfall in the Western North Pacific
566 and East Asian sector, *J. Clim.*, 22, 2073–2094, <https://doi.org/10.1175/2008JCLI2538.1>, 2009.

567 The Joint Typhoon Warning Center Tropical Cyclone Best-Tracks, 1945-2000:
568 <https://www.metoc.navy.mil/jtwc/products/best-tracks/tc-bt-report.html>, last access: 25June2019.

569 Curran, T. J., Brown, R. L., Edwards, E., Hopkins, K., Kelley, C., McCarthy, E., Pounds, E., Solan, R., and Wolf, J.:
570 Plant functional traits explain interspecific differences in immediate cyclone damage to trees of an endangered
571 rainforest community in north Queensland, *Austral Ecol.*, 33, 451–461, <https://doi.org/10.1111/j.1442->
572 9993.2008.01900.x, 2008.

573 Douglas, I.: Hydrological investigations of forest disturbance and land cover impacts in South–East Asia: a review,
574 *Philos. Trans. R. Soc. London. Ser. B Biol. Sci.*, 354, 1725–1738, <https://doi.org/10.1098/rstb.1999.0516>, 1999.

575 Dvorak, V. F.: Tropical cyclone intensity analysis using satellite data,
576 <https://repository.library.noaa.gov/view/noaa/19322>, 1984.

577 Dvorak, V. F., Smigielski, F. J., and States., U.: A workbook on tropical clouds and cloud systems observed in satellite
578 imagery, file://catalog.hathitrust.org/Record/002715963, 1990.

579 ECMWF: IFS Documentation CY45R1 - Part II : Data assimilation, in: IFS Documentation CY45R1, ECMWF,
580 <https://doi.org/10.21957/a3ri44ig4>, 2018.

581 ECMWF: ERA5-Land hourly data from 1981 to present, <https://doi.org/10.24381/cds.e2161bac>, 2019.

582 Eloy, C., Fournier, M., Lacoïnte, A., and Moulia, B.: Wind loads and competition for light sculpt trees into self-similar
583 structures, *Nat. Commun.*, 8, 1–11, <https://doi.org/10.1038/A41467s41467-017-00995-6>, 2017.

584 ESA: Land Cover CCI Product User Guide Version 2, 105pp., 2017.

585 Forzieri, G., Pecchi, M., Girardello, M., Mauri, A., Klaus, M., Nikolov, C., Rüetschi, M., Gardiner, B., Tomaščík, J.,
586 Small, D., Nistor, C., Jonikavicius, D., Spinoni, J., Feyen, L., Giannetti, F., Comino, R., Wolynski, A., Pirotti, F.,
587 Maistrelli, F., Savulescu, I., Wurpillot-Lucas, S., Karlsson, S., Zieba-Kulawik, K., Strejczek-Jazwinska, P., Mokroš,
588 M., Franz, S., Krejci, L., Haidu, I., Nilsson, M., Wezyk, P., Catani, F., Chen, Y.-Y., Luysaert, S., Chirici, G., Cescatti,
589 A., and Beck, P. S. A.: A spatially explicit database of wind disturbances in European forests over the period 2000–
590 2018, *Earth Syst. Sci. Data*, 12, 257–276, <https://doi.org/10.5194/essd-12-257-2020>, 2020.

591 [Grice, J. W.: Computing and evaluating factor scores., *Psychol. Methods*, 6, 430–450, https://doi.org/10.1037/1082-](https://doi.org/10.1037/1082-989X.6.4.430)
592 [989X.6.4.430](https://doi.org/10.1037/1082-989X.6.4.430), 2001.

593 Harris, I., Osborn, T. J., Jones, P., and Lister, D.: Version 4 of the CRU TS monthly high-resolution gridded
594 multivariate climate dataset, *Sci. Data*, 7, 1–18, <https://doi.org/10.1038/A41597s41597-020-0453-3>, 2020.

595 [Hersbach, H., Bell, B., Berrisford, P., Biavati, G., Horányi, A., Muñoz Sabater, J., Nicolas, J., Peubey, C., Radu, R.,
596 Rozum, I., Schepers, D., Simmons, A., Soci, C., Dee, D., Thépaut, J.-N. H. H., Bell, B., Berrisford, P., Biavati, G.,
597 and Horányi, A. J.-N.: ERA5 hourly data on single levels from 1959 to present. Copernicus Climate Change Service
598 \(C3S\) Climate Data Store \(CDS\), <https://doi.org/10.24381/cds.adbb2d47>, 2018.](https://doi.org/10.24381/cds.adbb2d47)

599 Honkavaara, E., Litkey, P., and Nurminen, K.: Automatic storm damage detection in forests using high-altitude
600 photogrammetric imagery, *Remote Sens.*, 5, 1405–1424, <https://doi.org/10.3390/rs5031405>, 2013.

601 [Jorge, S.-Z.: Copernicus Global Land Operations “Vegetation and Energy.”](#)
602 https://land.copernicus.eu/global/sites/cgls.vito.be/files/products/CGLOPS1_SQE2019_LAI300m-V1_I1.00.pdf
603 [2020.](#)

604 Kaplan, J. and Demaria, M.: On the decay of tropical cyclone winds after landfall in the New England Area, *J. Appl.*
605 *Meteorol.*, 40, 280–286, [https://doi.org/10.1175/1520-0450\(2001\)040<0280:OTDOTC>2.0.CO;2](https://doi.org/10.1175/1520-0450(2001)040<0280:OTDOTC>2.0.CO;2), 2001.

606 Kubota, H., Kosaka, Y., and Xie, S. P.: A 117-year long index of the Pacific-Japan pattern with application to
607 interdecadal variability, *Int. J. Climatol.*, 36, 1575–1589, <https://doi.org/10.1002/joc.4441>, 2016.

608 Landsea, C. W.: Climate variability of tropical cyclones: Past, Present and Future, in: *Storms*, edited by: Pielke, R. A.
609 S. and Pielke, R. A. J., Routledge, New York, 220–241, 2000.

610 Lin, T.-C., Hamburg, S., Lin, K.-C., Wang, L.-J., Chang, C.-T., Hsia, Y.-J., Vadeboncoeur, M. A., Mabry McMullen,
611 C. M., and Liu, C.-P.: Typhoon disturbance and forest dynamics: Lessons from a Northwest Pacific subtropical forest,
612 14, 127–143, <https://doi.org/10.1007/s10021-010-9399-1>, 2011.

613 Lin, T. C., Hogan, J. A., and Chang, C. Te: Tropical Cyclone Ecology: A Scale-Link Perspective, *Trends Ecol. Evol.*,
614 35, 594–604, <https://doi.org/10.1016/j.tree.2020.02.012>, 2020.

615 Louf, J. F., Nelson, L., Kang, H., Song, P. N., Zehnbaauer, T., and Jung, S.: How wind drives the correlation between
616 leaf shape and mechanical properties, *Sci. Rep.*, 8, 1–7, <https://doi.org/10.1038/A41598s41598-018-34588-0>, 2018.

617 Lu, Y., Yu, H., Yang, Q., Xu, M., Zheng, F., and Zhu, J.: Post-Disaster Survey of Typhoon Megi in Wenzhou City,
618 *Trop. Cyclone Res. Rev.*, 6, 34–39, <https://doi.org/10.6057/2017TCRRh1.04>, 2017.

619 ECMWF Confluence Wiki: Implementation of IFS cycle 45r1:
620 [https://confluence.ecmwf.int/display/FCST/Implementation+of+IFS+cycle+45r1#ImplementationofIFScycle45r1-](https://confluence.ecmwf.int/display/FCST/Implementation+of+IFS+cycle+45r1#ImplementationofIFScycle45r1-Tropicalcyclones)
621 [Tropicalcyclones.](#)

622 Mabry, C. M., Hamburg, S. P., Lin, ~~T. C.~~, [Teng-Chiu](#), Horng, F. W., King, H. B., and Hsia, Y. J.: Typhoon disturbance
623 and stand-level damage patterns at a subtropical forest in Taiwan, *Biotropica*, 30, 238–250,
624 <https://doi.org/10.1111/j.1744-7429.1998.tb00058.x>, 1998.

625 Martins, J. P., Trigo, I., and Freitas, S. C. de: Copernicus Global Land Operations ”Vegetation and Energy” “CGLOPS-
626 1,” *Copernicus Glob. L. Oper.*, 1–93, 2020.

627 McDowell, N. G., Allen, C. D., Anderson-Teixeira, K., Aukema, B. H., Bond-Lamberty, B., Chini, L., Clark, J. S.,
628 Dietze, M., Grossiord, C., Hanbury-Brown, A., Hurtt, G. C., Jackson, R. B., Johnson, D. J., Kueppers, L., Lichstein,
629 J. W., Ogle, K., Poulter, B., Pugh, T. A. M., Seidl, R., Turner, M. G., Uriarte, M., Walker, A. P., and Xu, C.: Pervasive
630 shifts in forest dynamics in a changing world, *Science* (~~80-~~), 368, <https://doi.org/10.1126/science.aaz9463>, 2020.

631 ~~Mei, W. and Xie, S. P.: Intensification of landfalling typhoons over the northwest Pacific since the late 1970s, *Nat.*
632 *Geosci.*, 9, 753–757, <https://doi.org/10.1038/ngeo2792>, 2016.~~

633 ~~NINO SST INDICES (NINO 1+2, 3, 3.4, 4; ONI AND TNI): [https://climatedataguide.ucar.edu/climate-data/nino-sst-](https://climatedataguide.ucar.edu/climate-data/nino-sst-indices-nino-12-3-34-4-oni-and-tni)
634 [indices-nino-12-3-34-4-oni-and-tni](https://climatedataguide.ucar.edu/climate-data/nino-sst-indices-nino-12-3-34-4-oni-and-tni), last access: 28February2019.~~

635 ~~Negrón-Juárez, R.-I., Baker, D. B., Zeng, H., Henkel, T. K., and Chambers, J. Q., Guimaraes, G., Zeng, H., Raupp,
636 C. F. M., Marra, D. M., Ribeiro, G. H. P. M., Saatchi, S. S., Nelson, B. W., and Higuchi, N.: Widespread Amazon~~

637 ~~forest.:~~ Assessing hurricane-induced tree mortality from a single cross-basin squall line event, in U.S. Gulf Coast
638 forest ecosystems, *J. Geophys. Res. Lett.*, **37**, 15, 115, G04030,
639 <https://doi.org/10.1029/2010GL043733>, 2010.

640 ~~Nelson, Negrón-Juárez, R., Baker, D. B. W., Kapos, V., Adams, Chambers, J. B., Oliveira, W. J., Braun, O. P. Q.,~~
641 ~~Hurt, G. C., and Amaral, I. L.:~~ ForestGoosem, S.: Multi-scale sensitivity of Landsat and MODIS to forest
642 disturbance by large blowdowns in the Brazilian Amazon, *Ecology*, **75**, 853–858, associated with tropical cyclones,
643 *Remote Sens. Environ.*, **140**, 679–689, <https://doi.org/10.2307/1941742>, <https://doi.org/10.1016/j.rse.2013.09.028>, 2014.

644 OCHA: Infrastructure Federation of Red Cross and Red Crescent Societies, Philippines : Typhoon Megi, 1–7pp., 2010.

645 Ozdogan, M., Vladimirova, N., Radeloff, V. C., Krylov, A., Wolter, P. T., and Baumann, M.: Landsat remote sensing
646 of forest windfall disturbance, *Remote Sens. Environ.*, **143**, 171–179, <https://doi.org/10.1016/j.rse.2013.12.020>, 2014.

647 ~~Revelle, R. W.:~~ psych, <https://cran.r-project.org/package=psych>, 2017.

648 Rustad, L. E., Campbell, J. L., Marion, G. M., Norby, R. J., Mitchell, M. J., Hartley, A. E., Cornelissen, J. H. C.,
649 Gurevitch, J., Alward, R., Beier, C., Burke, I., Canadell, J., Callaghan, T., Christensen, T. R., Fahnestock, J.,
650 Fernandez, I., Harte, J., Hollister, R., John, H., Ineson, P., Johnson, M. G., Jonasson, S., John, L., Linder, S., Lukewille,
651 A., Masters, G., Melillo, J., Mickelsen, A., Neill, C., Olszyk, D. M., Press, M., Pregitzer, K., Robinson, C., Rygiewicz,
652 P. T., Sala, O., Schmidt, I. K., Shaver, G., Thompson, K., Tingey, D. T., Verburg, P., Wall, D., Welker, J., and Wright,
653 R.: A meta-analysis of the response of soil respiration, net nitrogen mineralization, and aboveground plant growth to
654 experimental ecosystem warming, *Oecologia*, **126**, 543–562, <https://doi.org/10.1007/s004420000544>, 2001.

655 ~~Stuivenvolt Allen, J., Simon Wang, S. Y., LaPlante, M. D., and Yoon, J.:~~ Three Western Pacific Typhoons
656 Strengthened Fire Weather in the Recent Northwest U.S. Conflagration, *Geophys. Res. Lett.*, **48**,
657 <https://doi.org/10.1029/2020GL091430>, 2021.

658 Takao, G., Saigusa, N., Yamagata, Y., Hayashi, M., and Oguma, H.: Quantitative assessment of the impact of typhoon
659 disturbance on a Japanese forest using satellite laser altimetry, *Remote Sens. Environ.*, **156**, 216–225,
660 <https://doi.org/10.1016/j.rse.2014.09.028>, 2014.

661 Tang, S., Lin, T.-C., Hsia, Y.-J., Hamburg, S. P., and Lin, K.-C.: Typhoon effects on litterfall in a subtropical forest,
662 *Can. J. For. Res.*, **33**, 2184–2192, <https://doi.org/10.1139/x03-154>, 2003.

663 Therneau, T., Atkinson, B., and Ripley, B.: rpart: Recursive partitioning for classification, regression and survival
664 trees., CRAN R package version 4.1-15, 2019.

665 ~~The climate data guide: Nino SST indices (Nino 1+2, 3, 3.4, 4; ONI and TNI):~~
666 ~~Trenberth, K. E. and Stepaniak, D. P.:~~ Indices of El Niño evolution, *J. Clim.*, **14**, 1697–1701,
667 [https://doi.org/10.1175/1520-0442\(2001\)014<1697:LIOENO>2.0.CO;2](https://doi.org/10.1175/1520-0442(2001)014<1697:LIOENO>2.0.CO;2), 2001.

668 Uriarte, M., Thompson, J., and Zimmerman, J. K.: Hurricane María tripled stem breaks and doubled tree mortality
669 relative to other major storms, *Nat. Commun.*, **10**, 1–7, <https://doi.org/10.1038/A41467s41467-019-09319-2>, 2019.

670 Verger, A., Baret, F., and Weiss, M.: Near real-time vegetation monitoring at global scale, *IEEE J. Sel. Top. Appl.*
671 *Earth Obs. Remote Sens.*, **7**, 3473–3481, <https://doi.org/10.1109/JSTARS.2014.2328632>, 2014.

672 Vickers, B., Kant, P., Bleaney, A., Milne, S., Suzuki, R., Ramos, L. T., Pohnan, E., ~~and Lasee and Lasco~~, R. D.: Forests
673 and Climate Change Working Paper 7: Forests and Climate Change in the Asia-Pacific Region, Food and Agriculture
674 Organization of the United Nations, Rome, 1–126pp., 2010.

675 Virost, E., Ponomarenko, A., Dehandschoewercker, Quéré, D., and Clanet, C.: Critical wind speed at which trees break,
676 Phys. Rev. E, 93, <https://doi.org/10.1103/PhysRevE.93.023001>, 2016.

677 Wang, H.-C., Wang, S.-F., Lin, K.-C., Lee Shaner, P.-J., and Lin, T.-C.: Litterfall and Element Fluxes in a Natural
678 Hardwood Forest and a Chinese-fir Plantation Experiencing Frequent Typhoon Disturbance in Central Taiwan,
679 Biotropica, 45, 541–548, <https://doi.org/10.1111/btp.12048>, 2013.

680 Willoughby, H. E. and Rahn, M. E.: Parametric representation of the primary hurricane vortex. Part I: Observations
681 and evaluation of the Holland (1980) model, Mon. Weather Rev., 132, 3033–3048,
682 <https://doi.org/10.1175/MWR2831.1>, 2004.

683 WMO: Global Guide to Tropical Cyclone Forecasting, 399pp., 2017.

684 Xi, W.: Synergistic effects of tropical cyclones on forest ecosystems: a global synthesis, J. For. Res., 26,
685 <https://doi.org/10.1007/s11676-015-0018-z>, 2015.

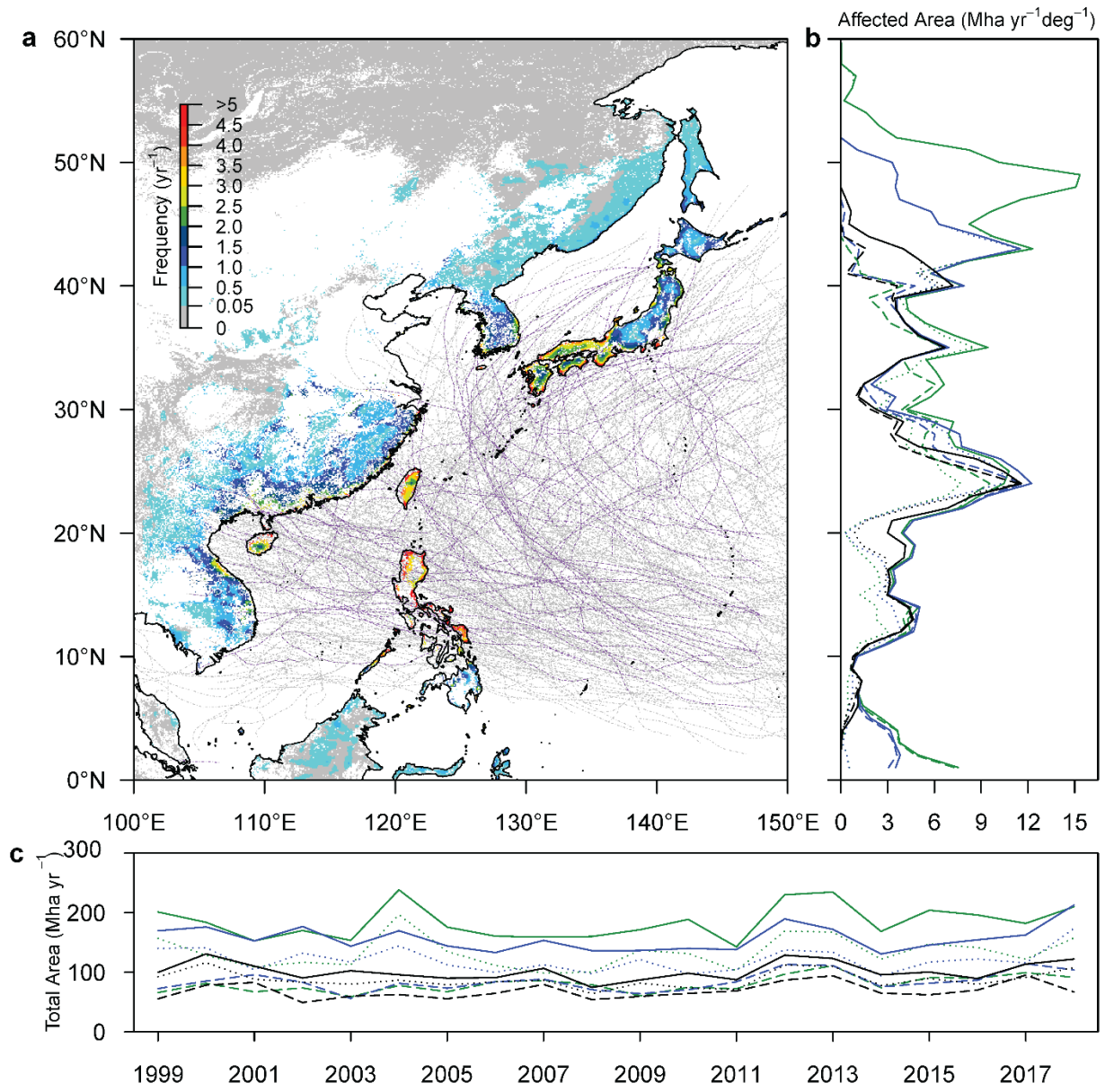
686 Yang, H.-H., Chen, S.-Y. C., Chien, S.-Y., and Li, W.-S.: Forensic Investigation of Typhoon Morakot Disaster:
687 Nansalu and Daniao Village Case Study (NCDR 102-T28), Taipei, 45pp., 2014.

688 Yoo, J., Kwon, H.-H. H., So, B.-J. J., Rajagopalan, B., and Kim, T.-W. W.: Identifying the role of typhoons as drought
689 busters in South Korea based on hidden Markov chain models, Geophys. Res. Lett., 42, 2797–2804,
690 <https://doi.org/10.1002/2015GL063753>, 2015.

691 ~~Zhao, T. and Dai, A.: Uncertainties in historical changes and future projections of drought. Part II: model simulated~~
692 ~~historical and future drought changes, Clim. Change, 144, 535–548, <https://doi.org/10.1007/s10584-016-1742-x>, 2017.~~

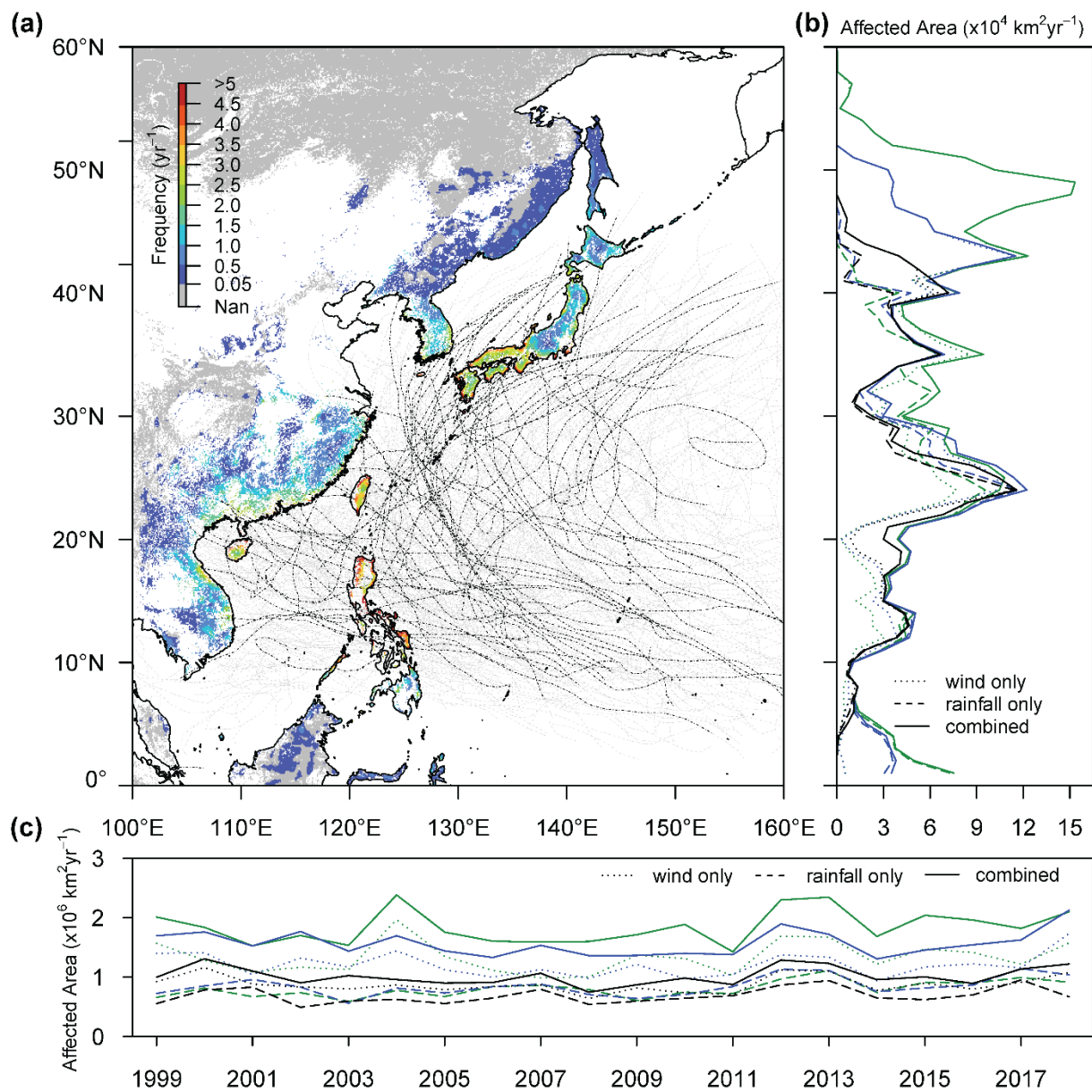
693

694



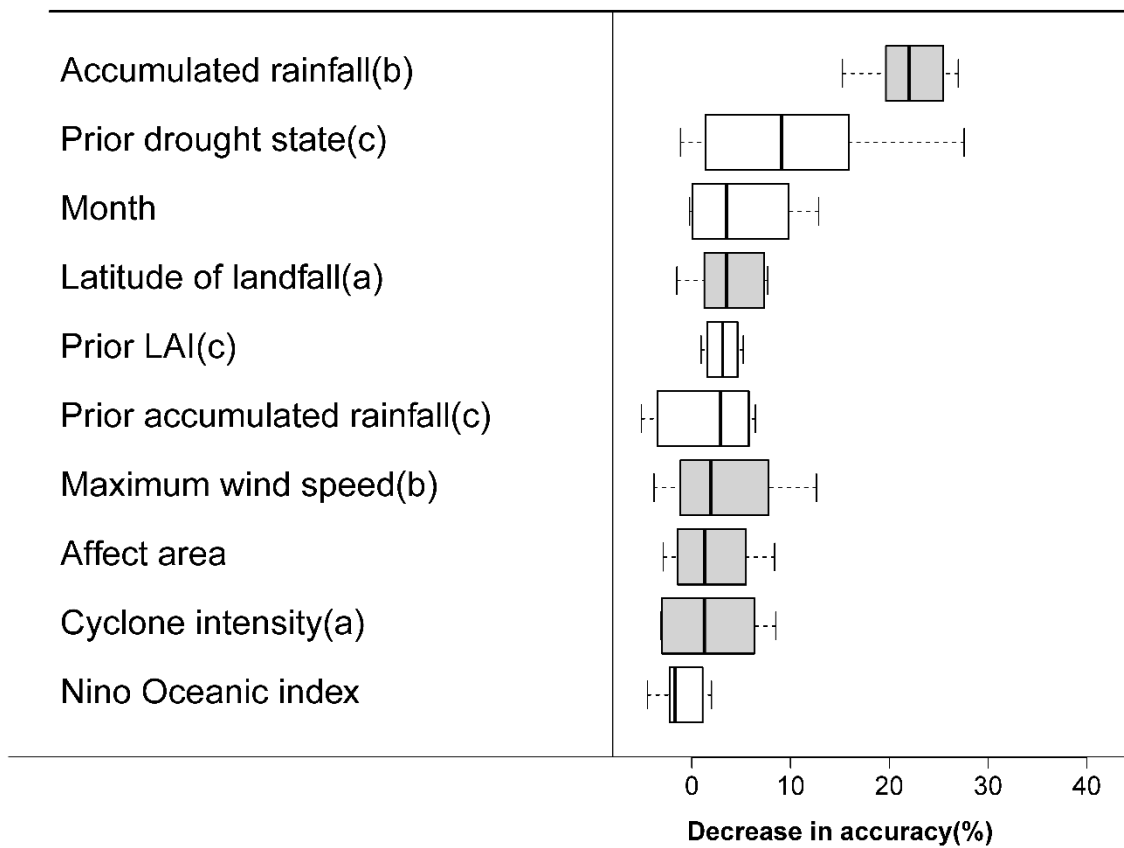
696

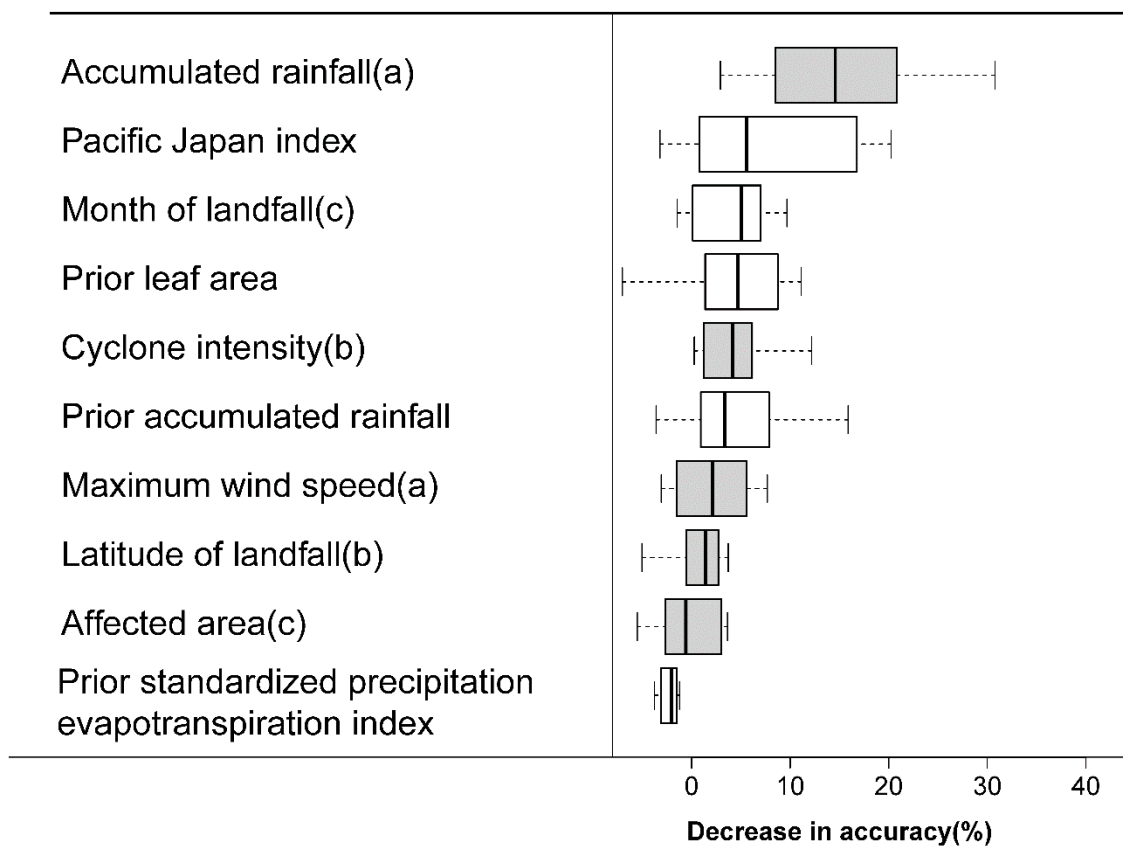
697



698
 699 **Figure 1.** Spatial and temporal patterns of potential forest damage by tropical cyclones in East Asia. **(Aa)** Return
 700 frequency (yr^{-1}) of tropical cyclones between 1999 and 2018. ~~Pixels where forest is the main land cover are shaded.~~
 701 ~~The color of the shading represents the return frequency of tropical cyclones based on-~~ following a combined wind-
 702 ~~precipitation~~ definition 3b for the affected area (considering three diameters to define the width of the storm track
 703 (definition 3a in Table A1). ~~Forests unlikely to have experienced a tropical cyclone between 1999 and 2018 are shaded~~
 704 ~~in grey.~~ For land locations shown in white, forest is not the dominant land cover. The dot-dashed lines show the
 705 cyclone tracks between 1999 and 2018. The ~~purpleblack~~ lines indicate the ~~easese~~ events that passed the QC/QA quality
 706 ~~control~~ criteria used in this study. **(B)** ~~Temporal dynamics of the total potentially damaged forest area (Mha yr^{-1}) for~~
 707 ~~all nine definitions of affected area.~~ **(C(b))** Latitudinal gradients of potentially damaged forest area ($\text{km}^2 \text{yr}^{-1}$) between

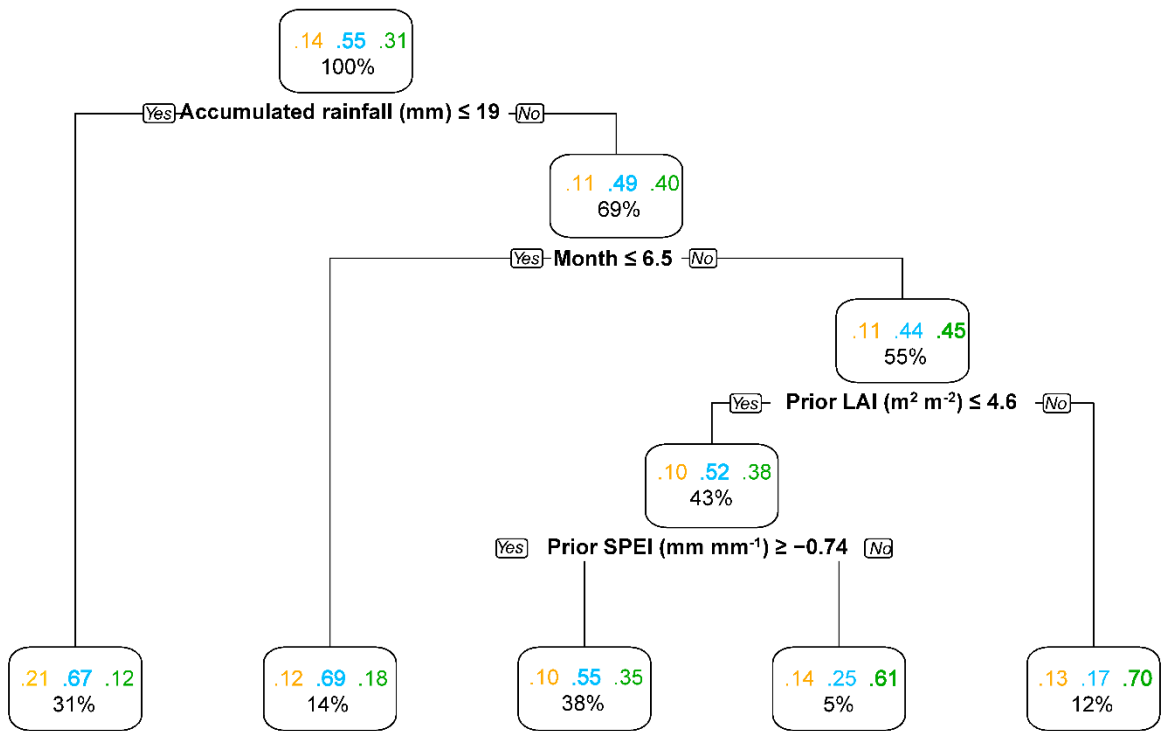
708 1999 to 2018 for all nine definitions of affected area. Damage potential is the outcome of an interplay between cyclone
709 frequency, cyclone intensity, and the presence of forests. The different definitions of affected area (Table A1)
710 consistently show a high potential for forest damage over island and coastal regions located between 10 and 35 degrees
711 north. This high potential is largely driven by the frequency of tropical cyclones (Fig. A1), i.e., two or more cyclones
712 making landfall per year. Depending on how the affected area is defined, there is a second region located between 40
713 and 50 degrees north with a high potential for storm damage. In this region, the potential damage is the outcome of
714 the high forest cover resulting in a strong dependency on the assumed width of the storm track (Fig. A1). $\text{Mha} \cdot \text{yr}^{-1} \cdot \text{deg}^{-1}$
715 between 1999 to 2018 (c) Temporal dynamics of the total potentially damaged forest area ($\text{km}^2 \cdot \text{yr}^{-1}$) for all nine
716 definitions of affected area. The dotted lines show the “wind only” definitions (group 1), the dashed lines show the
717 “rainfall only” definitions (group 2), and the solid lines show the “combined” definitions (group 3). The black, blue
718 and green colored lines represent definitions a, b and c, respectively, within each group. Definitions are detailed in
719 Table A1.
720

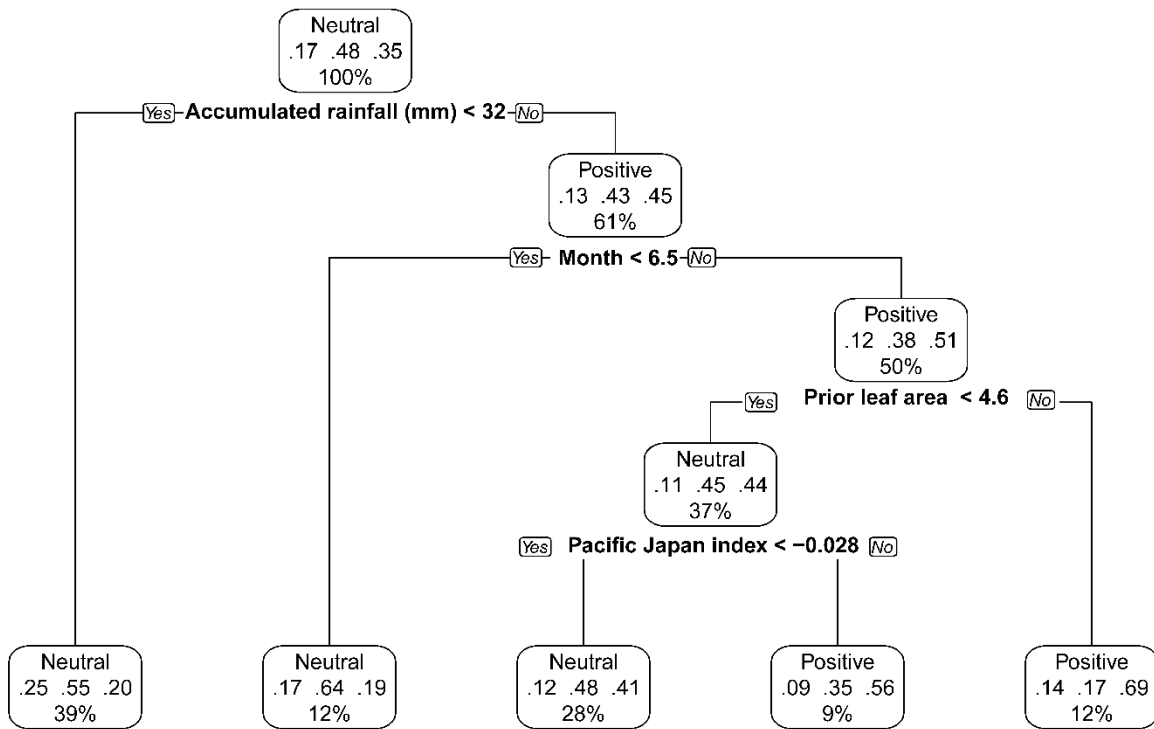




722
723
724
725
726
727
728
729
730
731

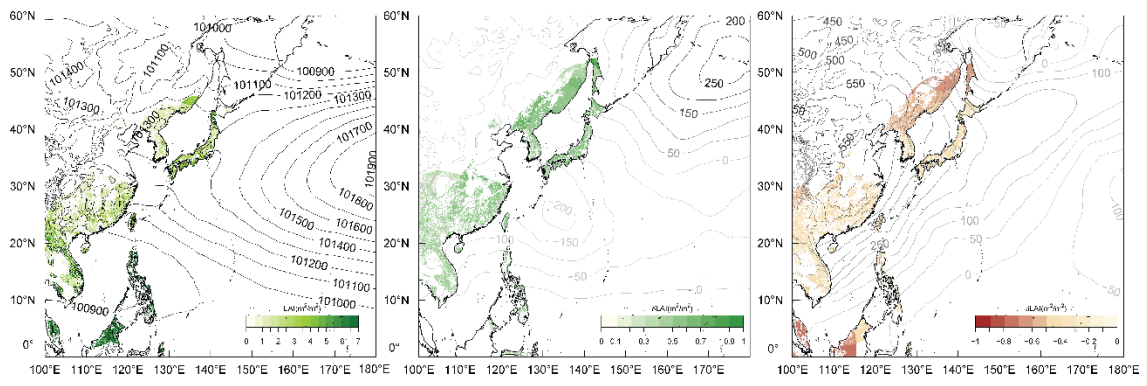
Figure 2. Importance of the five surface (white) and five cyclone (grey) characteristics in explaining the Leaf area response to the passage of a tropical cyclone. The boxplots show the 95, 75, 50, 25 and 5 percentiles of the decrease in accuracy. The letters a, b and c following the label of a characteristic indicate collinearity between the variables (Table A2). Each boxplot contains the results of 12 random forest analyses fitted with different combinations of largely uncorrelated characteristics (Table A3). Each random forest analysis is based on 13091262 cases coming from the 145 ± 42140 ± 41 individual tropical cyclones for which the impact was quantified according to nine related definitions (Table A1). The medians were used to sort the cyclone and surface characteristics according to decreasing importance.

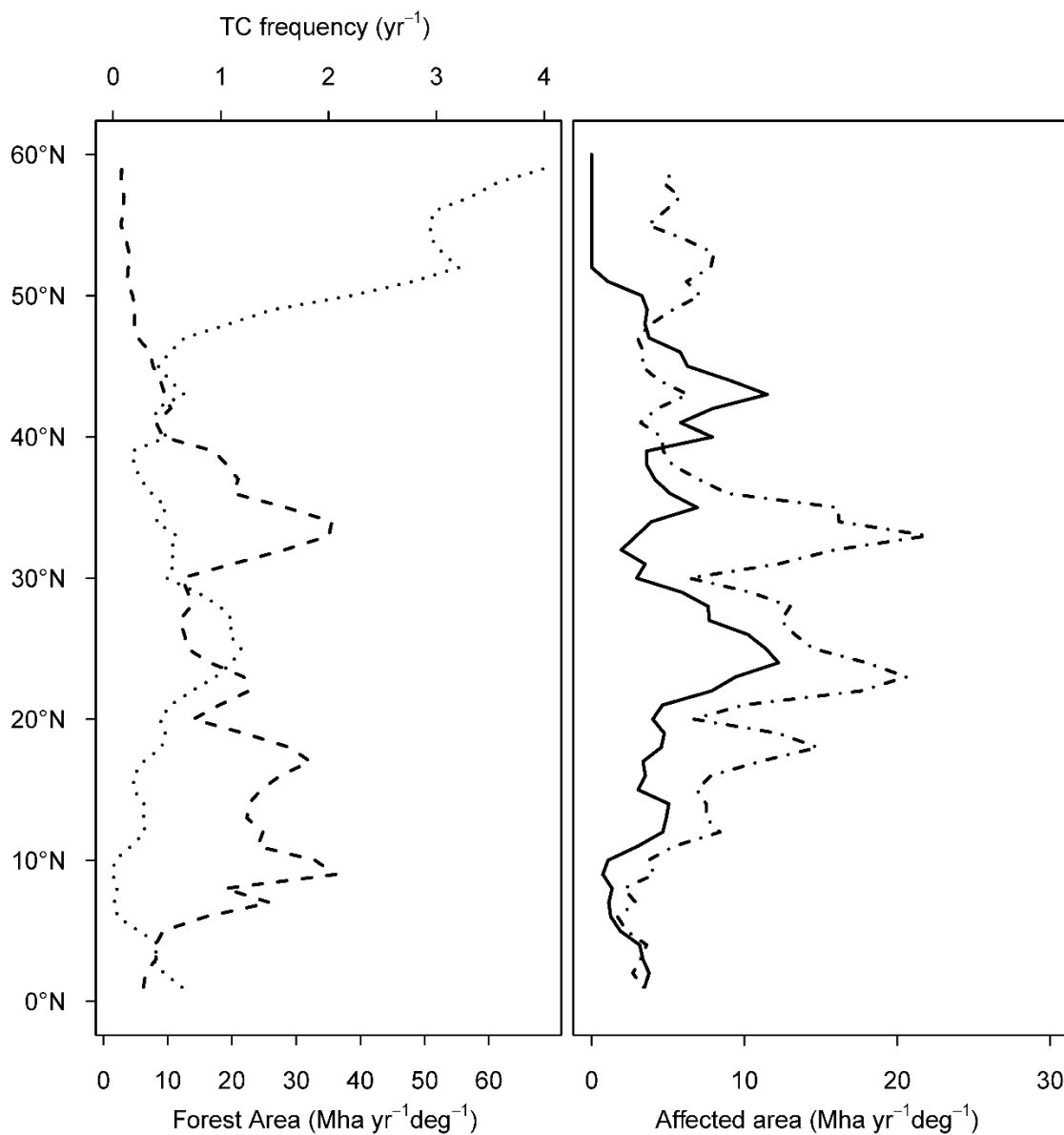




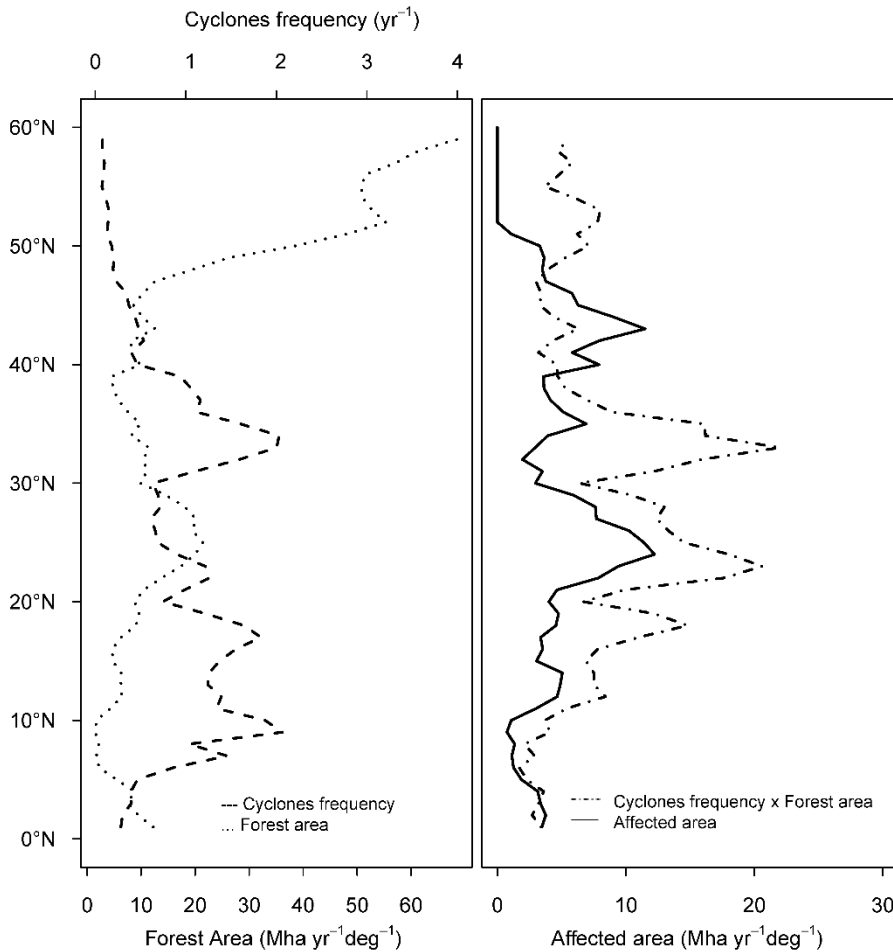
733
 734 **Figure 3.** Environmental drivers contributing to an increase of LAI in leaf area in the affected compared to the
 735 reference area, following the passage of a tropical cyclone. The fractions of a negative, (left), neutral (middle) and
 736 positive (right) effect size are listed for shown in each box in respectively orange, blue, and green. The number of
 737 events is listed as the percentage of the total number of events in the random tree (n=1309)-1262). To reduce the
 738 collinearity of the input variables, only the six variables with the highest accuracy (Fig. 2) were used to create the
 739 four-layer decision tree.

740
 741





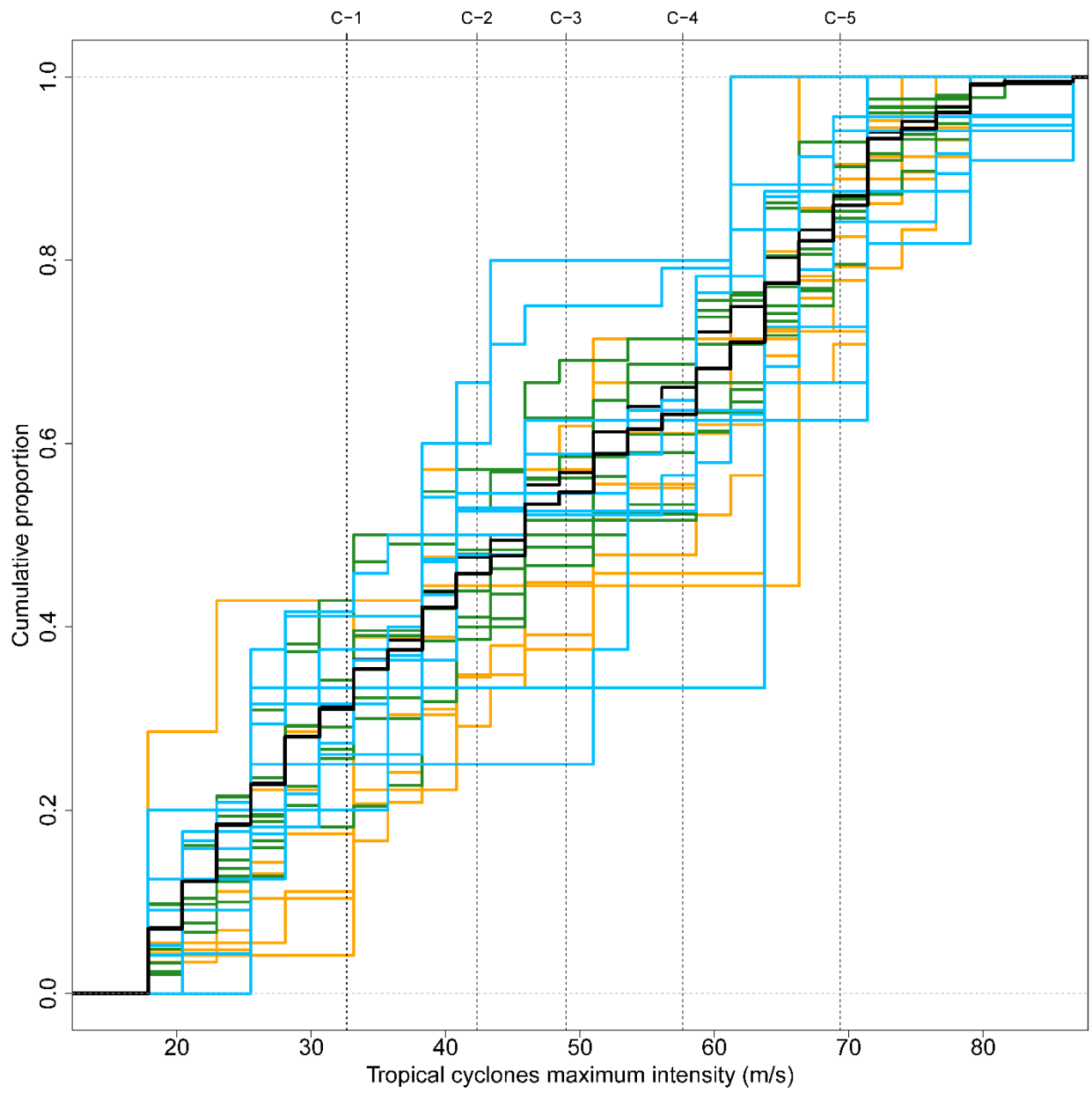
744
 745 **Figure 4.** Pressure fields (Pa) and changes therein in the month of the passage of a tropical cyclone for cyclones that
 746 had a neutral, positive, or negative impact on the leaf area ($\text{m}^2 \text{m}^{-2}$) of forests. Effect sizes are based on the definition
 747 that uses three times the cyclone diameter and wind speed to identify the affected and reference areas (definition 3a
 748 in Table A1) (a) Mean atmospheric pressure and leaf area prior to the passage of a tropical cyclone that had a neutral
 749 impact on forest leaf area. (b) Changes in mean atmospheric pressure and leaf area between cyclones with a neutral
 750 and positive effect on leaf area. (c) Changes in mean atmospheric pressure and leaf area between cyclones with a
 751 neutral and negative effect on leaf area.



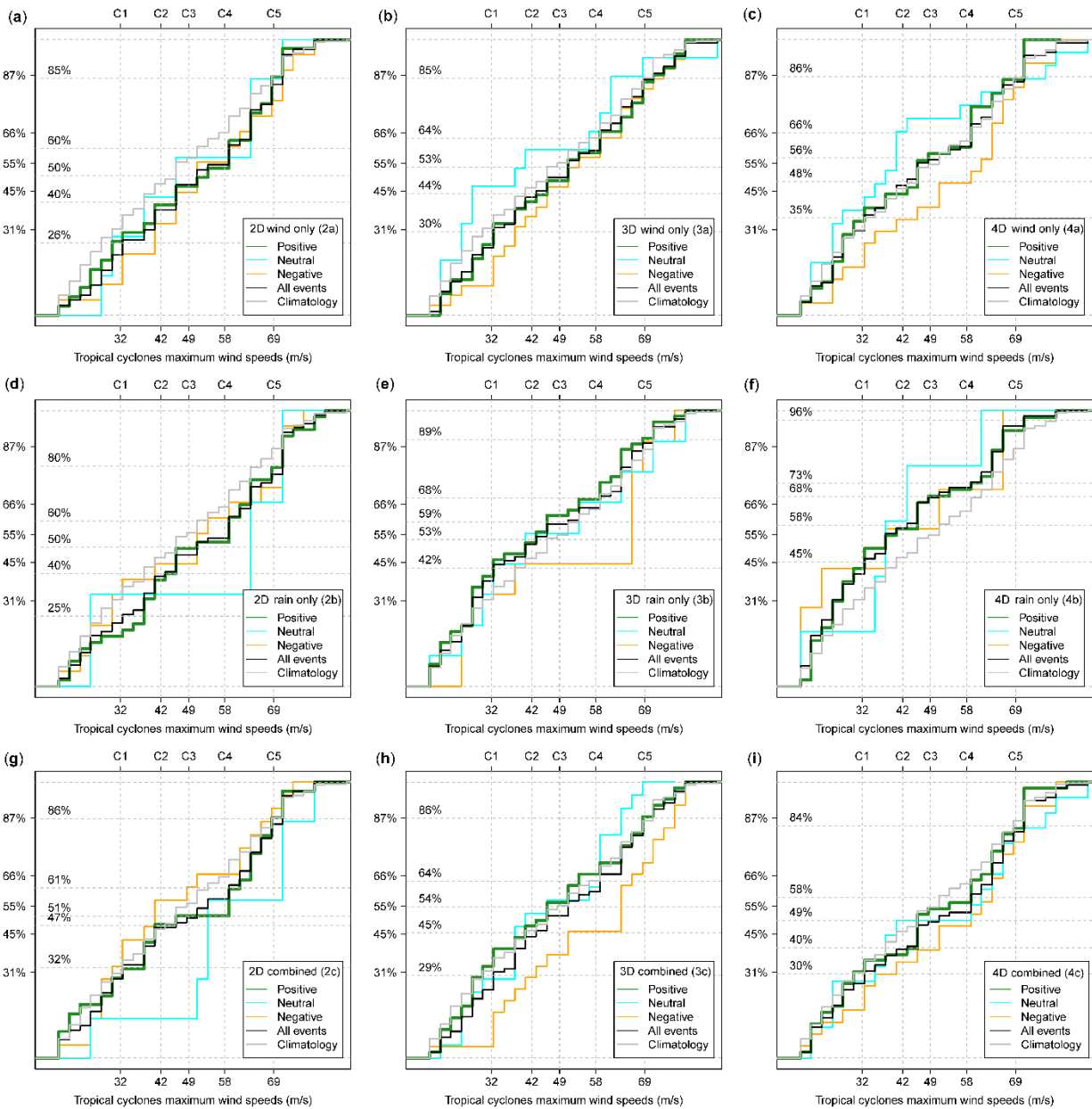
754

755 **Figure A1.** Contribution of return frequency and forest cover to the affected area: **(Aa)** zonal average of forest
 756 coverage (dotted line; $\text{Mha-deg}^{-1}\text{km}^2$) and the return frequency (dashed line; yr^{-1}) of **Tropical cyclones** from 0
 757 **degrees N** to 60 degrees N averaged over Eastern Asia, as defined in this study; **(Ab)** Zonal average of the
 758 interaction between return frequency and forest cover, calculated by multiplying the return frequency with the forest
 759 cover (dotdash line; $\text{Mhakkm}^2 \text{yr}^{-1} \text{deg}^{-1}$) and the estimated zonal average of the annual affected forest area (full line;
 760 $\text{Mhakkm}^2 \text{yr}^{-1} \text{deg}^{-1}$) for definition 3b (Table A1). Correlations between return frequency and affected area (Pearson
 761 correlation coefficient = -0.35, p-value < 0.01, n = 60), forest cover and affected area (Pearson correlation
 762 coefficient = 0.089, p-value = 0.5, n = 60) and frequency x cover and affected area (Pearson correlation coefficient =
 763 0.44, p-value < 0.01, n = 60). The latter thus correlates best with the zonal variation in the affected area and was
 764 therefore shown in subplot **B-b**. Results are shown for affected areas defined as locations within an area extending to
 765 three times the cyclone width for which the wind exceeded a threshold (definition 3a in Table S1)

766



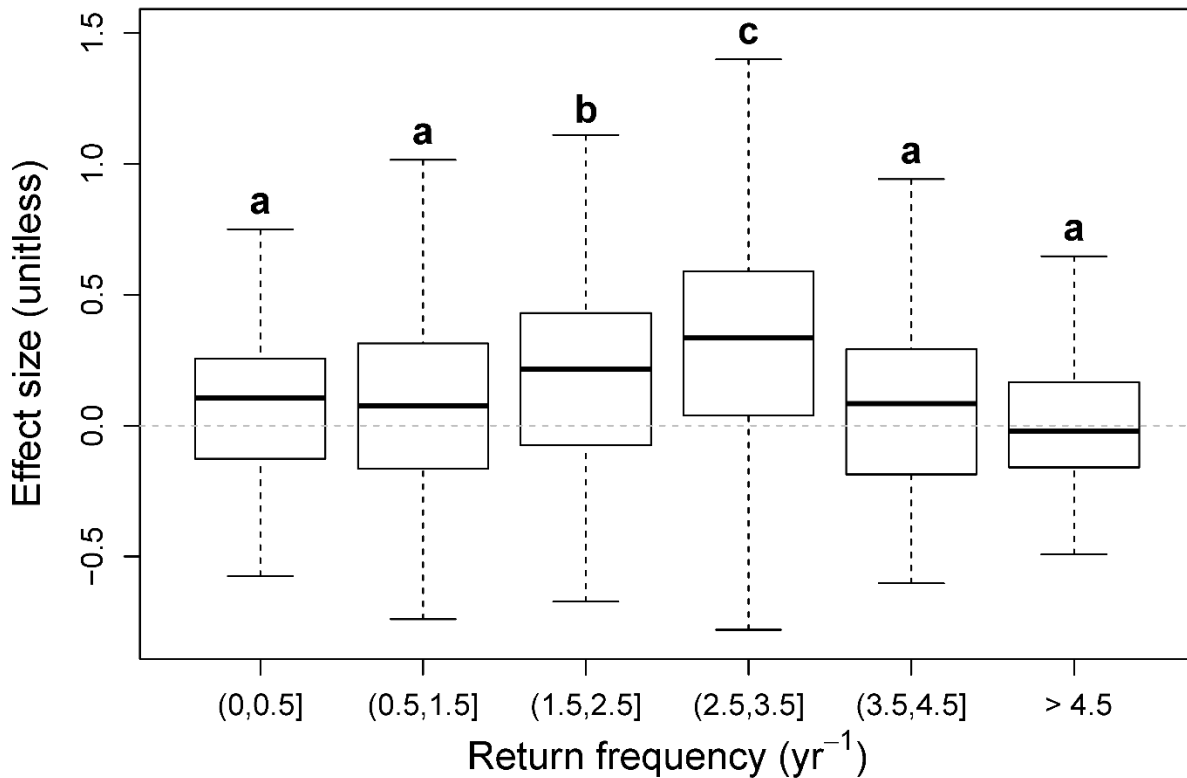
767
768



769

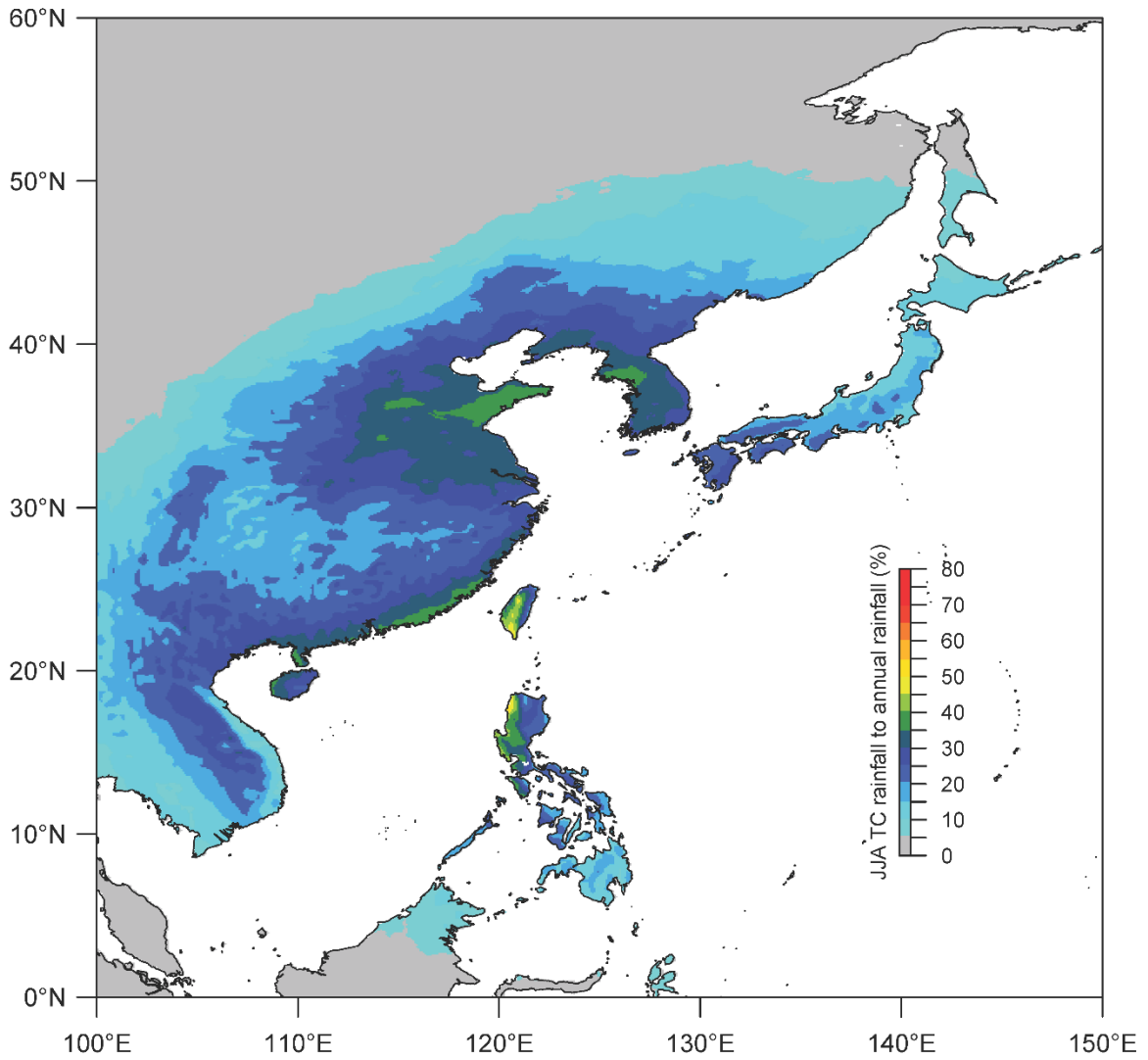
770 **Figure A2. Cumulative distribution function of the tropical cyclones as a function of their**
 771 **maximum intensity.** *The black solid line shows the distribution of the 580 events that occurred between 1999*
 772 *to 2018. The grey lines show the distributions obtained using all for the nine definitions to calculate the effect*
 773 *sizes of affected area used in this study. The cumulative distribution for the census of 580*
 774 *tropical cyclones recorded for the study period is shown left of the y-axis for class 1 (31%),*
 775 *class 2 (45%), class 3 (55%), class (4) 66% and class 5 (87%) cyclones. The numbers shown*
 776 *of the right of the y-axis represent the cumulative distribution of the sample of the 580*

777 events following a specific definition. Panel (a) shows wind only for 2 diameters, (b) wind
 778 only for 3 diameters, (c) wind only for 4 diameters, (d) rain only for 2 diameters, (e) rain
 779 only for 3 diameters, (f) rain only for 4 diameters, (g) wind or rain for 2 diameters, (h)
 780 wind or rain for 3 diameters, and (i) wind or rain for 4 diameters as detailed in Table S1.
 781 The intensity distribution for tropical cyclones with a negative effect size (is shown in
 782 orange); intensity distribution, for tropical cyclones with a neutral effect size (is shown in blue);
 783 and intensity distribution for tropical cyclones with a positive effect size (in green).
 784

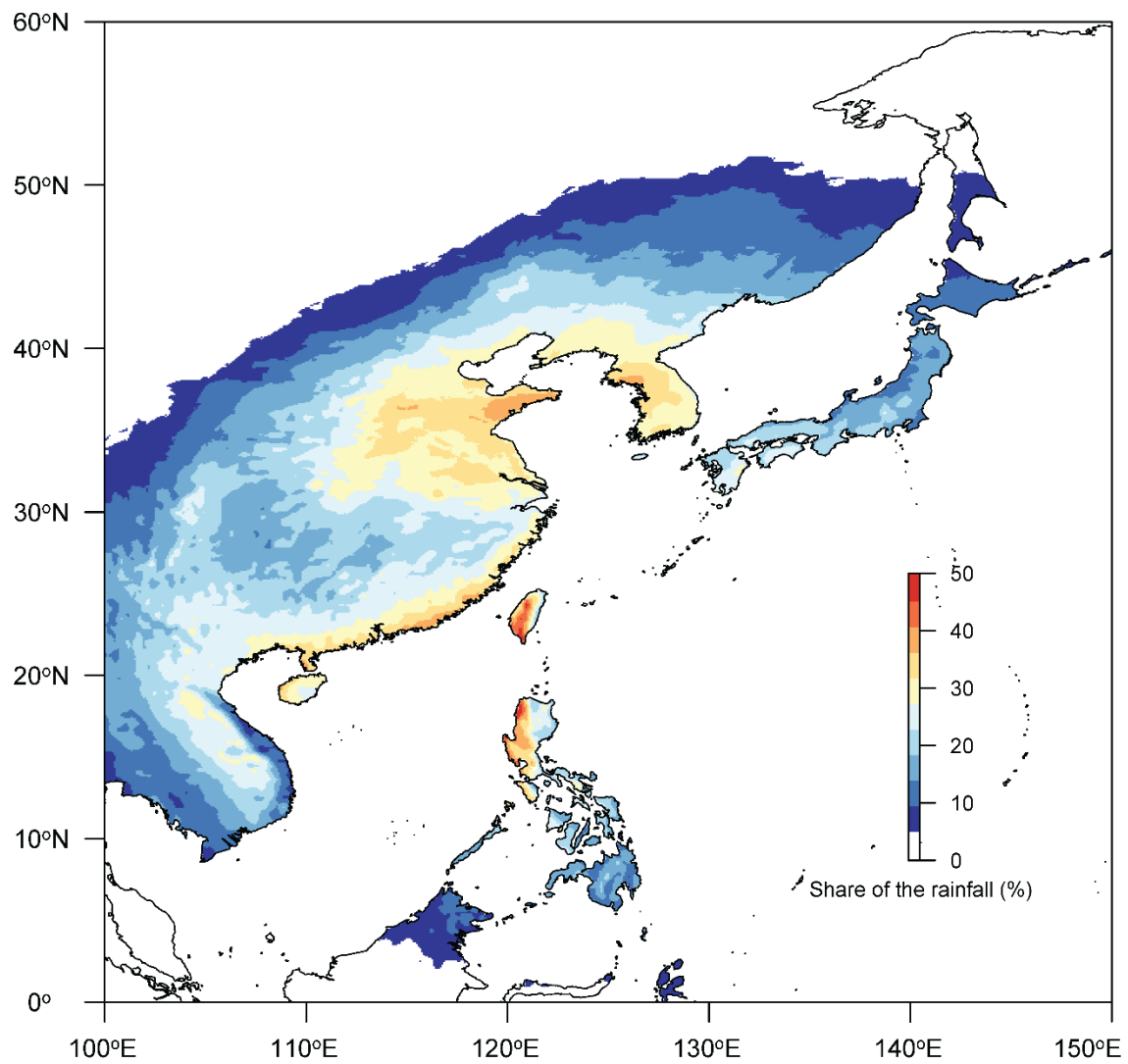


785 Figure A3. Box-and-whisker plots of the effect size. The black solid line shows the distribution for the specific definition
 786 (n = 140 ± 41 cyclones depending on LAI 60 days following the passage of a tropical cyclone stratified by the return
 787 frequency of the the definition). The grey solid line shows the distribution of the 580 events that occurred between
 788 1999 to 2018. Small deviations between the grey and the black line suggest that the sample well represented the 580
 789 cyclones in terms of their intensity class. The maximum wind speed of category 1 cyclones is between 32 m s⁻¹ and
 790 42 m s⁻¹, between 42 m s⁻¹ and 49 m s⁻¹ for category 2, between 49 m s⁻¹ and 58 m s⁻¹ for category 3, between 58 m s⁻¹
 791 and 70 m s⁻¹ for category 4.

792 ¹ and 69 m s⁻¹ for category 4, and exceeding 69 m s⁻¹ for category 5. In East Asia, tropical cyclones for the location
793 where the cyclone made landfall. The letters a, b and c on top of the box whiskers show the different groups
794 identified by a Tukey multiple comparison of intensity class 3 or higher are called typhoons.



795
796



797

798 **Figure A4A3.** Share (%) of the rainfall contributed by tropical cyclones in June, July and August (JJA) to the total
799 annual rainfall over Eastern Asia between 1999 to 2018.

800 **Table A1.** Criteria for distinguishing between the affected and reference areas following the passage of an individual
801 cyclone and the number of events according to each specific definition. Group 1 groups definitions based on wind
802 speed, group 2 definitions are based on precipitation and group 3 definitions are based on both wind speed and
803 precipitation. All three definitions include an estimate of storm path based on a multiple of the reported storm diameter.
804 Column A denotes the number of events for which data were lacking so that the effect size could not be calculated;
805 column B denotes the number of events for which all required data were available; column C denotes the subset of B
806 for which the data passed the quality control ~~(see Quality Control)~~; ES refers to effect size. A total of 580 unique
807 tropical cyclones were considered in this study.

Group	Affected area	Reference area	A	B	C	Negative ES effect size	Neutral ES effect size	Positive ES effect size
1.a	> 8 msm s ⁻¹ and <2 diameters	< 8 msm s ⁻¹ and <2 diameters	342	238	114 <u>105</u>	1922	6251	3332
1.b	> 10 msm s ⁻¹ and <3 diameters	< 10 msm s ⁻¹ and <3 diameters	305	275	188 <u>182</u>	3138	11397	4447
1.c	> 12 msm s ⁻¹ and <4 diameters	< 12 msm s ⁻¹ and <4 diameters	291	289	178 <u>183</u>	2731	10592	4660
2.a	> 60 mm and <2 diameters	< 60 mm and <2 diameters	338	242	117 <u>115</u>	1819	5551	4445
2.b	> 80 mm and <3 diameters	< 80 mm and <3 diameters	315	265	136 <u>129</u>	1011	6959	5759
2.c	> 100 mm and <4 diameters	< 100 mm and <4 diameters	311	269	888 <u>6</u>	79	3632	45
3.a	(> 8 msm s ⁻¹ or > 60 mm) and <2 diameters	(< 8 msm s ⁻¹ or < 60 mm) and < 2 diameters	352	228	105 <u>103</u>	2125	5045	3433
3.b	(> 10 msm s ⁻¹ or > 80 mm) and <3 diameters	(< 10 msm s ⁻¹ or < 80 mm) and < 3 diameters	304	276	196 <u>188</u>	2938	11495	5355
3.c	(> 12 msm s ⁻¹ or > 100 mm) and <4 diameters	(< 12 msm s ⁻¹ or < 100 mm) and < 4 diameters	288	292	187 <u>171</u>	2735	11083	5053
Mean			316	264	145 <u>140</u>	2125	7967	4548
Std			22	22	424 <u>1</u>	811	3125	810
Mean (%)			54	46	252 <u>4</u>	1418	5548	3134

Std (%)	4	4	7	68	218	67
808						
809						

810 **Table A2.** Loadings of each characteristic on three axes and collinearity between variables within the same group (See
811 ~~section “multivariate analysis” for more details~~). Collinearity was used to build random forests with largely
812 uncorrelated explanatory variables (**Fig. 2 & 3**). Factor analysis was performed separately for each group. Given the
813 exploratory nature of this analysis, a factor loading of 0.76 was used as a cut-off and those exceeding that level are
814 highlighted in bold face. ~~Here, TCC refers to characteristics describing the tropical cyclone itself and PC to the~~
815 ~~characteristics of the land and ocean prior to the cyclone.~~

816

Group	Characteristics	FC1	FC2	FC3	Collinearity
<u>TCC</u> Cyclone <u>characteristics</u>	Maximum wind speed during passage over land ($m s^{-1}$)	0.01	-0.79	0.21	a
	Accumulated rainfall during passage over land (mm)	-0.18	-0.83	-0.0803	ba
	Latitude of landfall (degrees)	0.83	0.04	0.1308	eb
	Intensity of the tropical cyclone, gusts ($m s^{-1}$)	0.87	0.14	0.06	eb
	Affected area during passage over land (ha)	0.15	0.09	0.97	dc
		-	=		dc
		0.123	0.010		
	Month of landfall	<u>5</u>	<u>6</u>	0.9072	
			-		ed
<u>PC</u> Surface <u>conditions</u> <u>prior to the</u> <u>cyclone</u>	Prior Accumulated accumulated rainfall (30 days prior to landfall (mm))	0.806	0.256		
		<u>2</u>	<u>0</u>	0.0217	
			=		e
	Prior Leaf area index leaf area index (30 days prior to landfall ($m^2 m^{-2}$))	0.828	0.230		
		<u>7</u>	<u>6</u>	-0.1507	
		-	=		f
	Oceanic Niño Prior Pacific Japan index the month of landfall ($K(Pa Pa^{-1})$)	0.026	0.960		
		<u>9</u>	<u>7</u>	0.0874	
	Prior drought state (SPEI standardized precipitation and evapotranspiration index , 30 days prior to landfall (mm mm ⁻¹))	0.170	-	0.3203	g
		<u>1</u>	0.719		
			<u>5</u>		

817

818
819
820
821
822
823

Table A3. Sets of largely independent variables that were used as input in the random forest analysis. Details of the variables are given in the section “multivariate analysis”. The justification for the groups is given by the collinearity as reported in Table S2. ~~LAI stands for leaf area index and SPEI stands for Standardized Precipitation Evapotranspiration Index.~~

<u>Set</u>	<u>Group with tropical cyclone characteristics (TC)</u>	<u>Group with land characteristics prior to the cyclone (PC)</u>
1	Maximum wind speed, affected area & latitude Maximum wind speed, cyclone intensity & affected area	Month & prior accumulated rainfall pre event LAI, oceanic Nino index & month
2	Accumulated rainfall, affected area & latitude	pre event LAI, oceanic Nino index & month
3	Accumulated rainfall, latitude & affected area Maximum wind speed, cyclone intensity & affected area	Prior Pacific Japan index & prior standardized precipitation and pre event LAI, oceanic Nino index & month
4	Accumulated rainfall, cyclone intensity & affected area Accumulated rainfall, cyclone intensity & affected area	pre event LAI, oceanic Nino index & month
5	Maximum wind speed, affected area & latitude affected area	pre event SPEI, oceanic Nino index & month
6	Accumulated rainfall, affected area & latitude	pre event SPEI, oceanic Nino index & month
7	Maximum wind speed, cyclone intensity & affected area	pre event SPEI, oceanic Nino index & month
8	Accumulated rainfall, cyclone intensity & affected area	pre event SPEI, oceanic Nino index & month
9	Maximum wind speed, affected area & latitude	pre event accumulative rainfall, oceanic Nino index & month
10	Accumulated rainfall, affected area & latitude	pre event accumulative rainfall, oceanic Nino index & month
11	Maximum wind speed, cyclone intensity & affected area	pre event accumulative rainfall, oceanic Nino index & month
12	Accumulated rainfall, cyclone intensity & affected area	pre event accumulative rainfall, oceanic Nino index & month